



Fall 2022

## Interrogating Antagonistic Differences Among *Pseudomonas Aeruginosa* Cdia Alleles

Haotian Yang

Follow this and additional works at: [https://ecommons.luc.edu/luc\\_theses](https://ecommons.luc.edu/luc_theses)



Part of the [Microbiology Commons](#)

---

### Recommended Citation

Yang, Haotian, "Interrogating Antagonistic Differences Among *Pseudomonas Aeruginosa* Cdia Alleles" (2022). *Master's Theses*. 4443.

[https://ecommons.luc.edu/luc\\_theses/4443](https://ecommons.luc.edu/luc_theses/4443)

This Thesis is brought to you for free and open access by the Theses and Dissertations at Loyola eCommons. It has been accepted for inclusion in Master's Theses by an authorized administrator of Loyola eCommons. For more information, please contact [ecommons@luc.edu](mailto:ecommons@luc.edu).



This work is licensed under a [Creative Commons Attribution-Noncommercial-No Derivative Works 3.0 License](#).  
Copyright © 2022 Haotian Yang

LOYOLA UNIVERSITY CHICAGO

INTERROGATING ANTAGONISTIC DIFFERENCES AMONG *PSEUDOMONAS*

*AERUGINOSA cdiA* ALLELES

A THESIS SUBMITTED TO

THE FACULTY OF THE GRADUATE SCHOOL

IN CANDIDACY FOR THE DEGREE OF

MASTER OF SCIENCE

PROGRAM IN INFECTIOUS DISEASE AND IMMUNOLOGY

BY

HAOTIAN YANG

CHICAGO, IL

AUGUST 2022

Copyright by Haotian Yang, 2022  
All rights reserved.

## ACKNOWLEDGEMENT

I would like to thank Mad Welt, Abigail Banas for their support of my graduate research work. I owe a special thanks to Dr. Allen for providing me with advices and skills that are necessary to finish my thesis project.

I would like to thank my thesis committee members, Dr. Visick, Dr. Kroken and Dr. Fitzpatrick for their advice.

## TABLE OF CONTENTS

ACKNOWLEDGEMENT .....	iii
LIST OF FIGURES .....	v
LIST OF TABLES .....	vi
LIST OF ABBREVIATIONS .....	vii
CHAPTER ONE: INTRODUCTION .....	1
CHAPTER TWO: MATERIAL AND METHODS .....	9
CHAPTER THREE: RESULT .....	18
CHAPTER FOUR: DISCUSSION .....	36
REFERENCE LIST.....	40
VITA.....	44

## LIST OF FIGURES

Figure 1. Current Model of Bacterial Contact-Dependent Growth Inhibition.....	6
Figure 2. <i>P. Aeruginosa</i> CdiA Is Highly Diverse.....	8
Figure 3. <i>P. Aeruginosa</i> Strains with CdiA-Tox3 Perform CDI under Standard Conditions.....	20
Figure 4. The CdiA-Tox3 Domain Is Predicted to Have Nucleotide Deaminase Activity.....	21
Figure 5. <i>P. Aeruginosa</i> Strains with CdiA-Tox5 Perform CDI under Standard Conditions.....	22
Figure 6. <i>P. Aeruginosa</i> Strains with CdiA-Tox11 Perform CDI under Standard Conditions....	23
Figure 7. The CdiA-Tox11 Domain Is Predicted to Have tRNase Activity.....	23
Figure 8. <i>P. Aeruginosa</i> Strains with CdiA-Tox12 Do Not Perform CDI under Standard Conditions.....	25
Figure 9. <i>P. Aeruginosa</i> Strains with CdiA-Tox10 Display Variable Competition Phenotypes.....	26
Figure 10. The CdiA-Tox10 Domain Is Predicted to Have Endonuclease Activity.....	27
Figure 11. Expression of <i>cdiA</i> Does Not Explain Competition Phenotypes.....	29
Figure 12. Heterologous CdiA <sup>BL017</sup> Toxin Expression but Not CdiA <sup>BL046</sup> Toxin Slows Bacterial Growth.....	31
Figure 13. Overexpression of the <i>cdi</i> Locus in BL046 Promotes CDI .....	32
Figure 14. BL022 Is Susceptible to CDI by a Different Strain with the Same Tox10 Domain.....	35

LIST OF TABLES

Table 1. Plasmids Used in This Study .....11

Table 2. Primers Used in This Study.....12

Table 3. Gene Fragments Used in This Study.....13

Table 4. Strains Used in This Study.....14

Table 5. Competition Assay Summary.....27

## LIST OF ABBREVIATIONS

CI	Competitive Index
Mbp	Megabase pair
RBD	Receptor binding domain



## CHAPTER ONE

### INTRODUCTION

#### ***Pseudomonas Aeruginosa* Is a Major Opportunistic Pathogen**

*Pseudomonas aeruginosa* is a gram-negative bacteria with a genome size of 5.5-7 Mbp[11]. The large genome of this organism provides flexibility and metabolic capabilities to survive in undesirable environments for most bacteria. *P. aeruginosa* is usually associated with respiratory tract infections and wound infections in a clinical setting. It is an opportunistic pathogen because it rarely causes infection in healthy individuals. Cystic Fibrosis (CF) Patients and immunocompromised individuals are at high risk of *P. aeruginosa* infection. CF is a genetic disorder that is caused by mutation of both copies of the CFTR gene. The airway of CF patients is covered by thick mucus which hinders the mucociliary clearance [11]. The high-salt environment in CF lung was also found to suppress the production of antimicrobial peptides [10]. Thus, the lung of CF patients is a favorable environment for bacterial colonization. *P. aeruginosa* is the predominant species that causes CF lung infections. Chronic infection of *P. aeruginosa* is associated with biofilm formation. The biofilm matrix is composed of LPS, neutrophil elastase inhibitor, DNA, which protect *P. aeruginosa* from the host immune system and antibiotic treatment. *P. aeruginosa* also mediates competition within CF lungs to shape biofilm structure. Besides biofilm, *P. aeruginosa* also encodes multiple secretion systems, quorum-sensing that contribute to its virulence. Immunocompromised patients who received a lung transplant and patients with HIV are more likely infected with *P. aeruginosa* [10]. Chemotherapy and selective

pressure of broad-spectrum antibiotics also increase the risk of *P. aeruginosa* infection because excessive use of antibiotics accelerates the development of multidrug-resistant strains. We study interbacterial competition to understand how a system used in bacterial competition may serve a role in the pathogenesis of *P. aeruginosa*.

### **Competitive Interactions among Bacteria**

Bacteria are complex social organisms that live within mixed communities where microorganisms including bacteria, viruses, and fungi interact. Members within a community can establish different relationships that are either cooperative or competitive. Cooperative interactions can benefit both parties (mutualism) or benefit only one partner without detriment to the other (commensalism). On the other hand, some interactions between microorganisms can be competitive. Competitive relationships can be categorized into exploitative and interfering [6]. Exploitative competition is a passive process in which one organism depletes nutrients in the surrounding so that its competitors don't have access to those resources. An example of exploitative competition occurs when bacteria secrete siderophores to chelate iron from their surrounding environment. This action limits the amount of iron available to neighboring bacterial competitors [6].

Interference competition requires an organism to produce antagonistic factors that directly kill or restrict the growth of competitors. Bacteria can take part in this type of antagonism through mechanisms that are contact-dependent or contact-independent. Contact-independent mechanisms use secreted factors that diffuse away from the producing cell to target competitors at a distance. Well-studied examples of contact-independent antagonistic factors include specialized metabolites (SM) such as antibiotics. At sufficient concentrations, antibiotics impart growth inhibition to susceptible bacteria; however, subinhibitory concentrations of antibiotics may trigger unique

responses from targeted bacteria to counteract the antibiotic-producing species. For instance, in response to subinhibitory antibiotics, *Bacillus subtilis* produces a lipopeptide surfactant called surfactin to form biofilms and facilitate some type of motility. Surfactin also antagonizes sporulation and aerial growth of antibiotic-producing *Streptomyces* spp [6]. Contact-dependent competition requires bacteria to be in close contact so that toxic effector modules can be directly delivered to targeted cells. Delivery of these effector modules can involve the type IV secretion system (T4SS), type V secretion system (T5SS), type VI secretion system (T6SS), Esx-Like Secretion System (ESS), or outer membrane exchange (OME)[12]. The mechanism of toxin module delivery by the T4SS and T6SS is better characterized than for the T5SS, ESS, and OME. Both T4SS and T6SS are large macromolecular complexes that function to secrete toxin molecules directly into eukaryotic and prokaryotic cells. The T4SS translocates toxins through a hollow needle structure that spans between two cells [13], while the T6SS acts as a molecular spear and forces attached toxins through the outer membrane of the target cell [14]. Traditionally, the T4SS was studied for its role in mediating F-plasmid conjugation but it was later observed that pathogens such as *Helicobacter pylori* can transfer protein toxins to host cells through T4SS [9]. Recently, *Xanthomonas* species was found to carry a T4SS that is specialized to transfer bacterial toxins into rival bacterial cells, resulting in cell death [9]. Likewise, the T6SS was first studied for its role in pathogenesis and later for its ability to transfer toxins required for bacterial competition. While most effectors specifically target either prokaryotic or eukaryotic cells, the T6SS effector Vgr2b was found to function as a zinc-metallopeptidase that can kill both prokaryotic and eukaryotic cells [15]. For toxin modules of both the T4SS and T6SS, specific immunity factors are encoded immediately downstream of the toxin genes that bind and neutralize the toxin to protect siblings during interbacterial competition [9].

### Contact-Dependent Growth Inhibition (CDI)

Contact-dependent growth inhibition (CDI) is a particular type of interference competition mediated by a T5SS complex. It was first identified in *E. coli* strain EC93 isolated from rat's gut. In a co-culture experiment of EC93 with lab strain *E. coli* K-12, EC93 was found to kill K-12. *E. coli* is known to produce soluble antimicrobial peptide colicin, but the inhibition was not associated with colicin because K-12 was not inhibited by EC93 filtered culture supernatants [2]. When EC93 and K-12 were separated by a 0.4-micron membrane, no inhibition was observed; however, separation of EC93 and K-12 by an 8-micron membrane resulted in suppression of K-12, suggesting that the inhibition requires cell-to-cell contact. It was subsequently determined that a three-gene cluster, *cdiBAI*, was responsible for the CDI inhibitory phenotype [2].

CdiB and CdiA make up a two-partner, or a type V<sub>b</sub>, secretion system [16]. Both CdiB and CdiA are secreted into the periplasm of Gram-negative bacteria through the SecYEG pathway. CdiB is a  $\beta$ -barrel protein that translocates CdiA across the outer membrane to the cell surface. CdiA is the actual effector protein that functions to deliver and release its C-terminal toxin domain into a targeted bacterium. The activity of this toxin domain can be either static or cidal, but ultimately antagonizes replication of the target cell. The final gene in the cluster, *cdiI*, encodes for an immunity factor that is produced to neutralize the CdiA toxin domain (Fig. 1A). This protects the producing cell or neighboring siblings from intoxication.

As stated, CdiA is exported to the cell surface of an attacking cell by its partner CdiB [2]. Export of CdiA proceeds from the amino terminus until a specific point at which secretion is halted (Fig. 1B). In this arrested state, the amino half of CdiA forms a rigid filament composed of a repeating filamentous hemagglutinin peptide sequence (FHA1, Pfam ID PF05594) that displays a receptor-binding domain (RBD) away from the cell surface. The carboxy half of CdiA remains

sequestered in the periplasm of the attacking cell, linked to the RBD through an extended secretion arrest (SA) domain [17]. Binding of the RBD to a specific outer-membrane receptor (OMR) on the target cell is an apparent trigger that resumes CdiA export and initiates the next phase of CDI (Fig. 1B) [17]. In *E. coli*, RBD variation between different *cdiA* alleles determines the specific OMR exploited on the surface of the target bacterium (PMID: 28351921).

In the second phase of CDI, the newly released carboxy domains of CdiA function to deliver the C-terminal toxin domain into the targeted bacterium (Fig. 1B). This begins when the FHA-2 domain (Pfam ID PF13332) of CdiA stably associates with the outer membrane of the targeted cell and facilitates translocation of the remaining carboxy domains into the periplasm through an unknown mechanism (Fig. 1B) [17]. During this translocation event, it is likely that these remaining carboxy domains are proteolytically cleaved and released into the target cell periplasm. Some CdiA-toxin domains function from within the periplasm by attacking the outer leaflet of the inner membrane [18]. Many others target nucleic acids and require another transport step across the inner membrane into the cytosol [19]. This is accomplished by an additional cytoplasmic entry (CE) domain encoded within these particular *cdiA* alleles. Specific inner membrane proteins (IMP) in a targeted cell are thought to tether the released carboxy domains (CE-Tox) near the inner membrane. There the CE domain facilitates translocation of the Tox domain across the inner membrane [19][20]. As with the RBD, CE variation between different *cdiA* alleles determines the specific IMP exploited for translocation of the toxin.

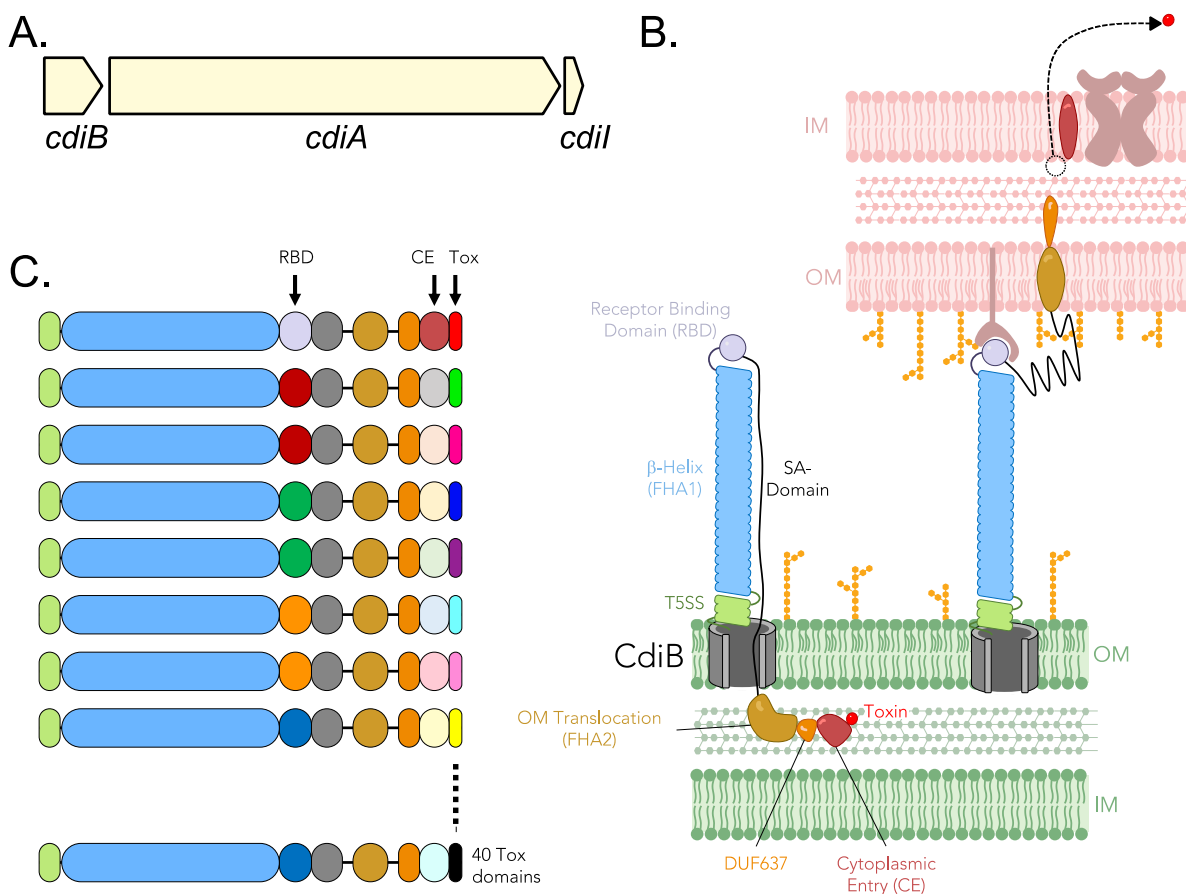


**Figure 1. Current Model of Bacterial Contact-Dependent Growth Inhibition.** (A) Gene order at the *cdi* locus. (B) Current model of the CdiA secretion arrested state (left) with complete toxin delivery following RBD engagement (right). (C) Cartoon of *P. aeruginosa* CdiA protein domains highlighting the diversity of the RBD, CE, and Tox domains. Original diagrams prepared by J. Allen

### CDI Toxin Diversity

Many protein toxins that promote interbacterial competition are composed of several domains where the N-terminal regions of the protein guide secretion and delivery of a C-terminal “toxin” domain (i.e., small effector domain) into a neighboring cell. Proteins described above are often polymorphic, meaning the same protein in a different bacterial strain may contain a different toxin domain [12]. Several studies have highlighted the diverse repertoire of polymorphic toxin

domains that exist within and across bacterial species [21][22]. Such toxin diversity can have dramatic effects on population dynamics in mixed microbial communities [23][24][25].

CdiA is a prime example of a polymorphic toxin that is highly diverse and effective at mediating interbacterial competition [26]. While many CdiA toxin domains have yet to be characterized, those that have been investigated display a diverse array of functions, including ionophores [18], tRNAses [27], DNAses [19], and Ribosomal RNAses [28]. Recent studies have revealed that some *cdiA* alleles are more potent than others, meaning that strains with those specific alleles perform better in competition [29]. *P. aeruginosa* also has a diverse armament of CdiA toxin domains (Fig. 2) [30][31][32][1], but their function and potency has not been studied. Thus, in this project we sought to elucidate the complexities of CDI in *P. aeruginosa* by investigating to what extent different *cdiA* alleles mediate interbacterial competition.

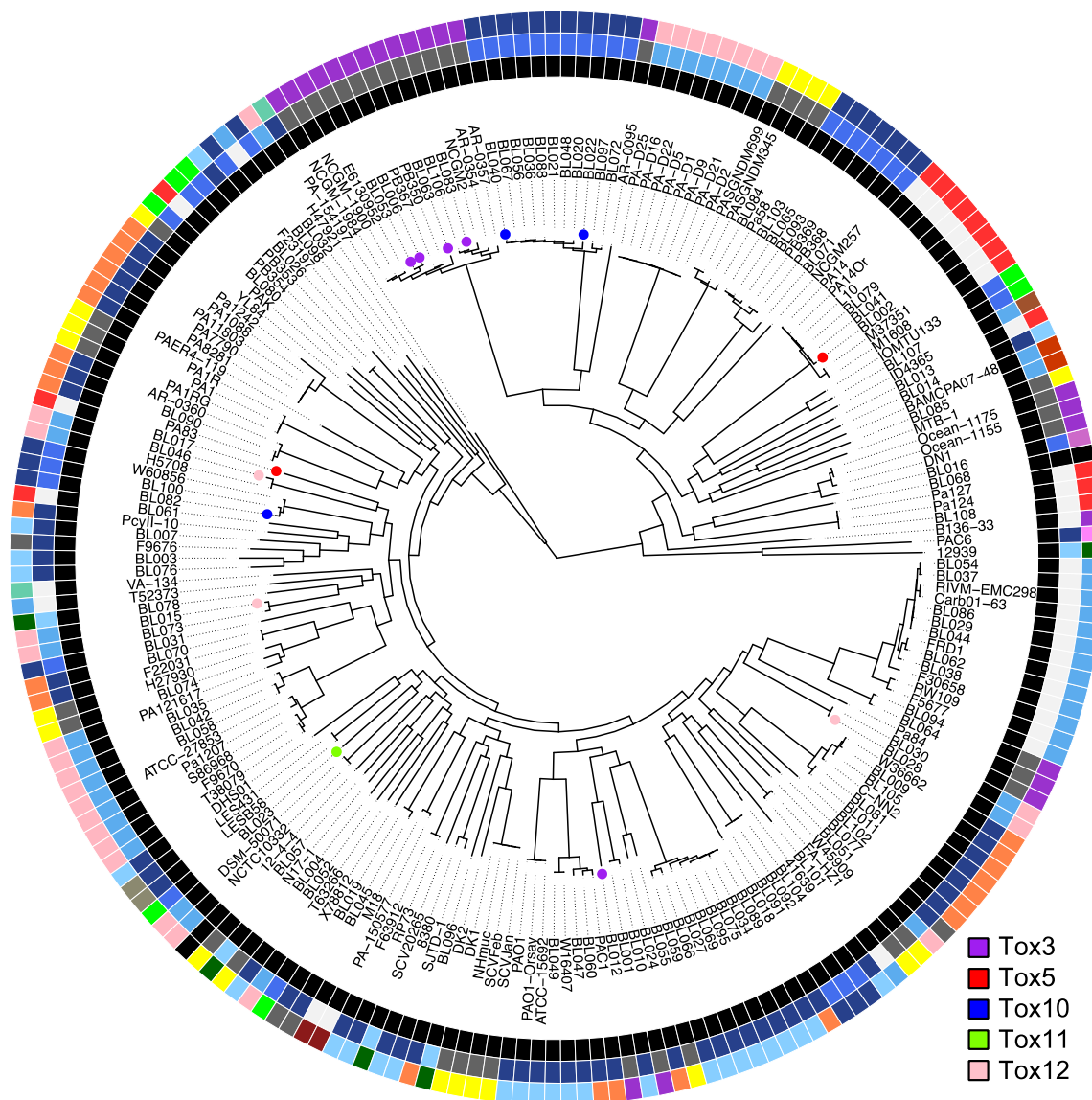


**Figure 2. *P. Aeruginosa* CdiA Is Highly Diverse.** Allelic diversity within the *cdiA* receptor-binding domain (inner ring), inner membrane translocation domain (middle ring), and carboxy-terminal toxin domain (outer ring) was mapped onto a maximum likelihood core genome tree containing over 200 *P. aeruginosa* strains. Ring colors represent different variants of the respective domains. Tree branches with dots at the tips reflect *P. aeruginosa* strains investigated in this study, colored according to their respective *cdiA* carboxy-terminal toxin allele (see legend). Adapted from Allen et al. [1]



## CHAPTER TWO

### MATERIALS AND METHODS

#### **Competition Assay**

Interbacterial competition assays were performed in accordance with previous studies [33]. Competing *P. aeruginosa* strains were individually subcultured 1:100 from overnight growth into 5 ml LB and incubated at 37°C with shaking until the OD<sub>600</sub> reached between 0.6 and 1.0. Subcultures were each concentrated to an OD<sub>600</sub> of 10. Concentrated strains were mixed at a 10:1 ratio of “attacking” and “target” strains respectively based on their experimental designation. Five microliter spots were placed in triplicate onto solid agar LB plates and incubated at 37°C for 3 hr to allow for interbacterial competition. The input ratio of attacking and target strains was determined by serial dilution and plating on selective media with overnight growth at 37°C. All target strains were engineered to encode a gentamicin resistance cassette located at the attTN7 site within the *P. aeruginosa* chromosome [43]. At 3hr, competition spots were harvested using an inverted 1ml pipette tip make an agar punch around the spot. Agar punches were placed in 1 ml LB and bacteria were removed from the punch by heavy vortexing. As with the bacterial input, the output ratio of attacking and target strains was enumerated by serial dilution and plating on selective media. Two individual experiments were performed for each strain and the technical replicates were performed in triplicates. A competitive index (CI) was calculated from the enumerated colony forming units (CFU), where  $CI = (\text{Target CFU}_{3\text{hr}} / \text{Attacking CFU}_{3\text{hr}})$

/ Attacking CFU<sub>3hr</sub>) ÷ (Target CFU<sub>0hr</sub> / Attacking CFU<sub>0hr</sub>). The limit of detection of this assay is 100cfu/spots.

### **Mutant Generation**

*P. aeruginosa* chromosomal deletions were generated using the procedure of Schweizer and colleagues (1) by members of the Allen lab. Briefly, cloning vectors were designed to generate allelic replacement constructs for creation of unmarked in-frame deletion mutants. (Table 1). Forward (F) and Reverse (R) primers were used to PCR amplify ~500 nucleotides of homologous sequence flanking the upstream (up) or downstream (dn) regions of the respective region of interest (Table 2). PCR fragments flanking the deletion target were combined using Gibson assembly into the EcoRI site of pEX18-GM. Assembled plasmids were transformed into NEB® 5-alpha Competent *E. coli* (New England Biolabs) for plasmid maintenance. Plasmids were introduced to *P. aeruginosa* by conjugation using *E. coli* S17.1 (2, 3). Merodiploids were isolated on LB plates supplemented with 100 µg/ml gentamicin and subsequently resolved by sucrose counter-selection. Final constructs were screened by replica plating for antibiotic susceptibility and confirmed by PCR and sequencing of the amplified fragment. All final mutant strains were confirmed by Sanger DNA sequencing of final PCR products through Genewiz. Insertion of a gentamicin resistance cassette into the att: TN7 chromosomal site was performed as described by Schweizer and colleagues using the plasmid pUC18TminiTn7Tgm [43]. Gene fragments encoding N-terminal polyhistidine-tagged CdiA1 Toxin domains and cognate C-terminal HA-tagged immunity factors were purchased from IDT (Table 3). Gene fragments were combined with the broad-host-range plasmid pSB109 cut with EcoRI by Gibson assembly and transferred to *P. aeruginosa* as described above.

**Table 1. Plasmids Used in This Study**

Plasmid	Primers/gene fragments used	Source
pEX18.gm		[33]
pUC18TminiTN7Tgm		[33]
pSB109		[33]
pEX18.gm BL002 cdiA1ΔToxΔcdiI	pEX18_BL002_CT05_Fup/Rup/Fdn/Rdn	This study
pEX18.gm BL006 cdiA1ΔToxΔcdiI	pEX18_BL006_CT05_Fup/Rup/Fdn/Rdn	This study
pEX18.gm BL012 cdiA1ΔToxΔcdiI	pEX18_BL012_CT05_Fup/Rup/Fdn/Rdn	This study
pEX18.gm BL015 cdiA1ΔToxΔcdiI	pEX18_BL046_CT05_Fup/Rup/Fdn/Rdn	This study
pEX18.gm BL028 cdiA1ΔToxΔcdiI	pEX18_BL046_CT05_Fup/Rup/Fdn/Rdn	This study
pEX18.gm BL040 cdiA1ΔToxΔcdiI	pEX18_BL022_CT05_Fup/Rup/Fdn/Rdn	This study
pEX18.gm BL022 cdiA1ΔToxΔcdiI	pEX18_BL022_CT05_Fup/Rup/Fdn/Rdn	This study
pEX18.gm BL023 cdiA1ΔToxΔcdiI	pEX18_BL023_CT05_Fup/Rup/Fdn/Rdn	This study
pEX18.gm BL046 cdiA1ΔToxΔcdiI	pEX18_BL046_CT05_Fup/Rup/Fdn/Rdn	This study
pEX18.gm BL053 cdiA1ΔToxΔcdiI	pEX18_BL006_CT05_Fup/Rup/Fdn/Rdn	This study
pEX18.gm BL063 cdiA1ΔToxΔcdiI	pEX18_BL006_CT05_Fup/Rup/Fdn/Rdn	This study
pEX18.gm BL083 cdiA1ΔToxΔcdiI	pEX18_BL006_CT05_Fup/Rup/Fdn/Rdn	This study
pSB109 BL017 6xHis-CdiA Tox	pSB109_17CdiA_Tox gene fragment	This study
pSB109 BL017 6xHis-CdiA Tox/CdiI-HA	pSB109_17CdiA_ToxIMM gene fragment	This study
pSB109 BL046 6xHis-CdiA Tox	pSB109_46CdiA_Tox gene fragment	This study
pSB109 BL046 6xHis-CdiA Tox/CdiI-HA	pSB109_46CdiA_ToxIMM gene fragment	This study

**Table 2. Primers Used in This Study**

Primer	Sequence (5'-3')
pEX18_BL002_CT05_FUP	CCGGGTACCGAGCTCGGGTAAGCCTCGTCGGTGAAA
pEX18_BL002_CT05_RUP	TTATTTTTTATGCTCTCATCCAACACTCCCCCTCCCCC
pEX18_BL002_CT05_FDN	AGGGGGAGTGTTGGATGAGAGCATAAAAAATAAAATAA
pEX18_BL002_CT05_RDN	ATGACCATGATTACGGGATATGGGTGGTTATTTCAG
pEX18_BL006_CT03_FUP	CGGGTACCGAGCTCGTTCTGGGCACGAATGCCTAC
pEX18_BL006_CT03_RUP	ATTTACGTTGAAACATCAACCCCACAACCCAAATCTAC
pEX18_BL006_CT03_FDN	TTTGGGTTGTGGGGTTGATGTTTTCAACGTAAATGAAAT
pEX18_BL006_CT03_RDN	ATGACCATGATTACGACATTC AATAGCACCACGCC
pEX18_BL022_CT10_FUP	CGGGTACCGAGCTCGAGACCCACAAGCTGGAAACC
pEX18_BL022_CT10_RUP	TTATTGAAAACAACATCACCCCTTGCGGAGCCGGCAGCT
pEX18_BL022_CT10_FDN	CCGGCTCCGCAAGGGTGATGTTGTTTTCAATAAAAAATA
pEX18_BL022_CT10_RDN	ATGACCATGATTACGAGTTCTCTTTGGCATTGTTT
pEX18_BL023_CT11_FUP	CGGGTACCGAGCTCGAGGACTCAACGAAGCACTGG
pEX18_BL023_CT11_RUP	AGAAACAGCGTTACATCAACCTTGCGGAGCCGGCAGCT
pEX18_BL023_CT11_FDN	CCGGCTCCGCAAGGTTGATGTAACGCTGTTTCTTCGCT
pEX18_BL023_CT11_RDN	ATGACCATGATTACGCGTTGATTGCCCGTCAGTTG
pEX18_BL046_CT12_FUP	CGGGTACCGAGCTCGGGGAAAATGGTAGGTGGCGA
pEX18_BL046_CT12_RUP	TACCTTTTGCCCCAATCATTTTCGGACCATCCGTAACGA
pEX18_BL046_CT12_FDN	ACGGATGGTCCGAAATGATTGGGGCAAAGGTAGCTCC
pEX18_BL046_CT12_RDN	ATGACCATGATTACGCGTTGATTGCCCGTCAGTTG
pEX18_BL012_CT03_FUP	CGGGTACCGAGCTCGGAGCTTCCTCGCCCTATGTG
pEX18_BL012_CT03_RUP	ATTTACGTTGAAACATCAACCCCACAACCCAAATCTAC
pEX18_BL012_CT03_FDN	TTTGGGTTGTGGGGTTGATGTTTTCAACGTAAATGAAAT
pEX18_BL012_CT03_RDN	ATGACCATGATTACGGGTA AACCCTCGCCCTTG
RpoD_qPCR FWD Set 3	GGGCGAAGAAGGAAATGGT
RpoD_qPCR REV Set 3	CTGGATCAGGTCGAGGAATTG
RpoD_qPCR PRB Set 3	/56-FAM/TCCATCGCC/ZEN/AAGAAGTACACCAACC/3IABkFQ/
GyrA_qPCR FWD Set 4	TCGCGAGCAGATTATCATCAC
GyrA_qPCR REV Set 4	CCCTCGATCTTCTTCTTTTTCAC
GyrA_qPCR PRB Set 4	/56-FAM/AAGGCGCGG/ZEN/TTGATCGAGAAGATC/3IABkFQ/
17CdiTox_qPCR FWD Set 3	GGAGTTTCGACCTACTATGAATGA
17CdiTox_qPCR REV Set 3	AGTTCCATCTAGATTCAGCCTAAC
17CdiTox_qPCR PRB Set 3	/56-FAM/AAGCGTCTG/ZEN/ATAGATGGTCGTGGG/3IABkFQ/
63CdiTox_qPCR FWD Set 4	ATCGAGTGGACGCAAAGATAG
63CdiTox_qPCR REV Set 4	GCCTTCTGAATAACGCCAATC
63CdiTox_qPCR PRB Set 4	/56-FAM/CCGAATGGG/ZEN/AATATGGCGGATGCT/3IABkFQ/
46CdiTox_qPCR FWD Set 1	AGTGCTTGATGCCTACCATAC

**Table 3. Gene Fragments Used in This Study**

Gene Fragment	Sequence 5'-3'
pSB109_17 CdiA_Tox	GCCGCGCGGCAGCCATATGGaaTCGAACGCTACTTTTGGTCAAATTA AAAACAGTGC TTGATACTGCGCAGGCTCCATATAAAGGTAGTACTGTTATAGGACATGCGCTATCT AAACATGCGGGTAGGCATCCCCGAAATATGGGGTAAAGTTAAAGGTTCTATGTCTG GTTGGAACGAACAAGCTATGAAGCATTTTAAGGAAATTGTCCTGCTCCTGGGGA GTTTCGACCTACTATGAATGAAAAGGGAATAACTTTTTAGAGAAGCGTCTGATA GATGGTCGTGGGGTTAGGCTGAATCTAGATGGAAC TTTTAAAGGGTTTATTGACT GAcctgcagtaccgtacgacg
pSB109_17 CdiA_ToxImm	GCCGCGCGGCAGCCATATGGaaTCGAACGCTACTTTTGGTCAAATTA AAAACAGTGC TTGATACTGCGCAGGCTCCATATAAAGGTAGTACTGTTATAGGACATGCGCTATCT AAACATGCGGGTAGGCATCCCCGAAATATGGGGTAAAGTTAAAGGTTCTATGTCTG GTTGGAACGAACAAGCTATGAAGCATTTTAAGGAAATTGTCCTGCTCCTGGGGA GTTTCGACCTACTATGAATGAAAAGGGAATAACTTTTTAGAGAAGCGTCTGATA GATGGTCGTGGGGTTAGGCTGAATCTAGATGGAAC TTTTAAAGGGTTTATTGACT GATGAAAGAATTATTTGAAGTGATTTTTGAGGGTGTGAACACTAGTAGGCTTTTTT TTCTTTTAAAAGAGATTGAAAGCAAGAGTGATCGCATTTTGGATTTTAAATTTTCT GAAGATTTTTTAGCTCTAATGTTAATGTTTTAGTGAATTATTGATCGATTCTTTC TTGGGTTTTAATGGTGATTTATTTTTGGTGTGTCCATGGAAGGGTTCAGTGTTAA GGATGGTTTGAAGTTGCCAGTCGTTCTCTTAAGGGTTTTGAAATATGAGGGGGGG GTTGATGTGGGGTTGTGTTTTATATGAATGATTTAATAGCGCAGGTAAGTTAT GTTAGAATTTCAAAAATATATGAATGGAATCTCTGCTGATTTTGGTTTCGAAAAT TCTATGGAGGTTTGGAGCCAGCCTCGGACCAAGAGACTAGGTTTTTTACTAACAA CAGGCTGGGTCTCTCTTTAGcctgcagtaccgtacgacg
pSB109_46 CdiA_Tox	GCCGCGCGGCAGCCATATGGaaCCGAAAGGAATACTTACACTGAAAGATTTTCCTG ATGTCTCTACCAAGATAAGCCAGAAGCAGCTTCGCCATATTGCTGGAACACAGCA GCTTGAGGCACGGGGAGGCGGTGGTTTCTTAAACAGTGTCTCTGATGCTCAAAAA GTGCTTGATGCCTACCATAACCGCCAAGTGAAAATCCTAGGGAGAAATGCTCAGG GATTCCCAGTAGTCAAGTTTGAAGGCGTTACTGGAAC TAACGTTAATCTCGGTGTT GGTATAACTGATCAGGCAACCAATGTATTTATTATCAAGGGCACAAAGAGTCCAA GTATTGTCCCTACAAATCCAAACTGGAGTCCCAAATGAcctgcagtaccgtacgacg
pSB109_46 CdiA_ToxImm	GCCGCGCGGCAGCCATATGGaaCCGAAAGGAATACTTACACTGAAAGATTTTCCTG ATGTCTCTACCAAGATAAGCCAGAAGCAGCTTCGCCATATTGCTGGAACACAGCA GCTTGAGGCACGGGGAGGCGGTGGTTTCTTAAACAGTGTCTCTGATGCTCAAAAA GTGCTTGATGCCTACCATAACCGCCAAGTGAAAATCCTAGGGAGAAATGCTCAGG GATTCCCAGTAGTCAAGTTTGAAGGCGTTACTGGAAC TAACGTTAATCTCGGTGTT GGTATAACTGATCAGGCAACCAATGTATTTATTATCAAGGGCACAAAGAGTCCAA GTATTGTCCCTACAAATCCAAACTGGAGTCCCAAATGAGTAGCCAGCCAACGTTG GAAGAATGGAATTTCAAGTGTTAATGCTAATTCAAGCGTTGGTAGGTGCGATAT CTGCCAATTTTAGAATGATTGCATGTTATGGGATGGCGATGAGTGGGTATTGAG ATTTTATCTTGAAGAGAGCAACGAAGAGGACGTTGAGGAGATTGAGGATGTTGTT TGCCAATATACGGCATATCAGGGCTCTAGTTTGAAGATGCAGGTCTGAGTTGATCGT GGGGCGTGAACGCCTTCCGGGGCTTTCGGAGGTGGGTAGGGTTGTATACCGTCCG AGAGAGTCTTTTGATATTTAGcctgcagtaccgtacgacg
pSB109_17 CdiA_Tox	GCCGCGCGGCAGCCATATGGaaTCGAACGCTACTTTTGGTCAAATTA AAAACAGTGC TTGATACTGCGCAGGCTCCATATAAAGGTAGTACTGTTATAGGACATGCGCTATCT AAACATGCGGGTAGGCATCCCCGAAATATGGGGTAAAGTTAAAGGTTCTATGTCTG GTTGGAACGAACAAGCTATGAAGCATTTTAAGGAAATTGTCCTGCTCCTGGGGA GTTTCGACCTACTATGAATGAAAAGGGAATAACTTTTTAGAGAAGCGTCTGATA GATGGTCGTGGGGTTAGGCTGAATCTAGATGGAAC TTTTAAAGGGTTTATTGACT GAcctgcagtaccgtacgacg

**Table 4. Strains Used in This Study**

Strain	Description	Source
BL002	Clinical Blood Stream Isolate	[33]
BL006	Clinical Blood Stream Isolate	[33]
BL012	Clinical Blood Stream Isolate	[33]
BL015	Clinical Blood Stream Isolate	[33]
BL028	Clinical Blood Stream Isolate	[33]
BL040	Clinical Blood Stream Isolate	[33]
BL022	Clinical Blood Stream Isolate	[33]
BL023	Clinical Blood Stream Isolate	[33]
BL046	Clinical Blood Stream Isolate	[33]
BL053	Clinical Blood Stream Isolate	[33]
BL063	Clinical Blood Stream Isolate	[33]
BL083	Clinical Blood Stream Isolate	[33]
BL002 cdiA1 $\Delta$ Tox $\Delta$ cdiI	CdiA1 Toxin and Immunity mutant	this study [MW]
BL006 cdiA1 $\Delta$ Tox $\Delta$ cdiI	CdiA1 Toxin and Immunity mutant	this study [MW]
BL012 cdiA1 $\Delta$ Tox $\Delta$ cdiI	CdiA1 Toxin and Immunity mutant	this study [HY]
BL015 cdiA1 $\Delta$ Tox $\Delta$ cdiI	CdiA1 Toxin and Immunity mutant	this study [MW]
BL028 cdiA1 $\Delta$ Tox $\Delta$ cdiI	CdiA1 Toxin and Immunity mutant	this study [MW]
BL040 cdiA1 $\Delta$ Tox $\Delta$ cdiI	CdiA1 Toxin and Immunity mutant	this study [MW]
BL022 cdiA1 $\Delta$ Tox $\Delta$ cdiI	CdiA1 Toxin and Immunity mutant	this study [MW]
BL023 cdiA1 $\Delta$ Tox $\Delta$ cdiI	CdiA1 Toxin and Immunity mutant	this study [MW]
BL046 cdiA1 $\Delta$ Tox $\Delta$ cdiI	CdiA1 Toxin and Immunity mutant	this study [MW]
BL053 cdiA1 $\Delta$ Tox $\Delta$ cdiI	CdiA1 Toxin and Immunity mutant	this study [MW]
BL063 cdiA1 $\Delta$ Tox $\Delta$ cdiI	CdiA1 Toxin and Immunity mutant	this study [MW]
BL083 cdiA1 $\Delta$ Tox $\Delta$ cdiI	CdiA1 Toxin and Immunity mutant	this study [MW]
BL002 cdiA1 $\Delta$ Tox $\Delta$ cdiI att:Tn7 GM	CdiA1 Toxin and Immunity mutant, Gm	this study [MW]
BL006 cdiA1 $\Delta$ Tox $\Delta$ cdiI att:Tn7 GM	CdiA1 Toxin and Immunity mutant, Gm	this study [MW]
BL012 cdiA1 $\Delta$ Tox $\Delta$ cdiI att:Tn7 GM	CdiA1 Toxin and Immunity mutant, Gm	this study [HY]
BL015 cdiA1 $\Delta$ Tox $\Delta$ cdiI att:Tn7 GM	CdiA1 Toxin and Immunity mutant, Gm	this study [MW]
BL028 cdiA1 $\Delta$ Tox $\Delta$ cdiI att:Tn7 GM	CdiA1 Toxin and Immunity mutant, Gm	this study [MW]
BL040 cdiA1 $\Delta$ Tox $\Delta$ cdiI att:Tn7 GM	CdiA1 Toxin and Immunity mutant, Gm	this study [MW]
BL022 cdiA1 $\Delta$ Tox $\Delta$ cdiI att:Tn7 GM	CdiA1 Toxin and Immunity mutant, Gm	this study [MW]
BL023 cdiA1 $\Delta$ Tox $\Delta$ cdiI att:Tn7 GM	CdiA1 Toxin and Immunity mutant, Gm	this study [MW]
BL046 cdiA1 $\Delta$ Tox $\Delta$ cdiI att:Tn7 GM	CdiA1 Toxin and Immunity mutant, Gm	this study [MW]
BL053 cdiA1 $\Delta$ Tox $\Delta$ cdiI att:Tn7 GM	CdiA1 Toxin and Immunity mutant, Gm	this study [MW]
BL063 cdiA1 $\Delta$ Tox $\Delta$ cdiI att:Tn7 GM	CdiA1 Toxin and Immunity mutant, Gm	this study [MW]
BL083 cdiA1 $\Delta$ Tox $\Delta$ cdiI att:Tn7 GM	CdiA1 Toxin and Immunity mutant, Gm	this study [MW]

### **Modeling of the CdiA-Toxin Domain**

Amino acid sequences from the different CdiA-Toxin domains were obtained from Allen et al., [1]. These were used as input for protein modeling using the SWISS-MODEL server (<https://swissmodel.expasy.org/interactive>) [35]. Images from the predicted structural models were generated with PyMOL (<https://pymol.org/2/>).

### **RNA Isolation**

Overnight cultures were grown in 5mL LB and incubated at 37C with shaking. Each strain was subcultured 1:10 from the overnight culture into 5mL LB in triplicates. The subcultures were incubated at 37C with shaking until the OD<sub>600</sub> reached between 0.6 and 0.8. 1mL of each subculture was harvested and was resuspended in 300μL PBS. To stabilize bacterial RNA, each sample was added with 1ml RNAProtect Bacteria Reagent and mixed by vortexing. After incubating for 5 min at room temperature, cells were harvested and lysed with a mixture of 20μL of QIAGEN Proteinase K in 200μL Lysozyme Buffer. Cell pellets were resuspended by pipetting and heavy vortexing. The mixtures were incubated at room temperature for 10 min to ensure that cells were fully lysed. RNA isolation was performed using the QIAGEN RNeasy mini Kit per manufacturers instructions. After the final RNA elution step, an additional DNase I digest step was added to remove residual gDNA. Each sample was treated with a mixture of 2.5μL DNase I and 10μL RDD buffer. The final volume was adjusted to 100μL and incubated for 10 to 15 min at room temperature. The remaining RNA was extracted by ethanol precipitation.

### **cDNA Synthesis**

RNA concentration and purity were assessed by UV absorbance (260nm/280nm) and gel electrophoresis. The cDNA was synthesized using the Thermo Superscript™ Master Mix and RNA template. Each reaction consisted of 4μL Superscript™ Master Mix and 2000 ng RNA. A No RT control of each sample also consisted of 4μL Superscript™ Master Mix without RT and 2000 ng RNA. The reaction mixtures were incubated at 25°C for 10 min, 50°C for 10 min, and 85°C for 5 min. The cDNA from this reaction was directly used for the quantitative PCR.

### **Quantitative PCR**

A single RT-PCR reaction consisted of 10μL Taqman® Fast Advanced Master Mix, 1.8 μL of forward and reverse primer and 0.5 μL probe. The final volume of the mixture was adjusted to 18.5 μL with nuclease free water. PCR reaction master mix was prepared using appropriate primers and probes. 18.5μL of master mix was added into each well of a MicroAmp® Fast 96-well reaction plate (0.1mL). 1.5μL cDNA or no template control were added to appropriate wells. The qPCR cycling conditions 50 °C for 2 min, 95 °C for 2 min, followed by 40 cycles of 95 °C for 5 sec. For each experiment, 3 biological replicates and processed in triplicates for technical replicates. The expression of *cdiA* relative to *rpoD* was quantified using the method of Livak and Schmittgen [34]

### **Western Blot**

The overnight cultures with *E.coli* NEBa that contain pMMB67 CdiA1 His-Tox/Imm-HA constructs were grown in 5mL LB (Amp50). The overnight cultures were subcultured 1:10 in 5mL LB (Amp50). The subcultures were grown at 37C with shaking for 1hr and then added IPTG to



1mM until  $OD_{600}$  reached 1.0. Subcultured *E.coli* was concentrated to  $OD=10$ . 1mL of the induced cultures were centrifuged down and resuspended with 100  $\mu$ L of Laemmli Buffer. Those samples were stored under -20C. On the day of running the gel, the samples were heated in 95C water bath for 5 min. 20  $\mu$ L of each sample were loaded and ran on 12% SDS Polyacrylamide gel. The gel was transferred to a nitrocellulose membrane. The membrane was blocked in 5% milk 1x TBS for 2hr and then probed with mouse anti-His antibody (1:2000) overnight at 4C. On the second day, the membrane was washed 3 times with TBS and probed with anti-mouse-AP conjugated antibody for 2hr at room temperature. The membrane was washed 3 times and developed with AP substrate.

### **Growth Curve**

The overnight cultures of *E.coli* NEBa that contain appropriate pMMB67 CdiA1 His-Tox/Imm-HA constructs were incubated at 37 C with shaking. The overnight culture was spun down and normalized to  $OD_{600} \sim 10$ . The growth curve was measured using a Costar 96-well plate. Each well of the 96-well plate was filled with 180 $\mu$ L LB (Amp50). 20 $\mu$ L normalized culture was added to the wells that correspond to various induction conditions. Each induction condition was measured in triplicates. Then, the plate was incubated in the plate reader for 3hr at 37°C with shaking. The plate reader measured  $OD_{600}$  every 15 min. After 3hr, the plate was taken out, induced with various amounts of IPTG, and put back with the same condition. The plate reader took  $OD_{600}$  reading every 15 min overnight. The data was plot on a grape as Time vs.  $OD_{600}$ .

## CHAPTER THREE

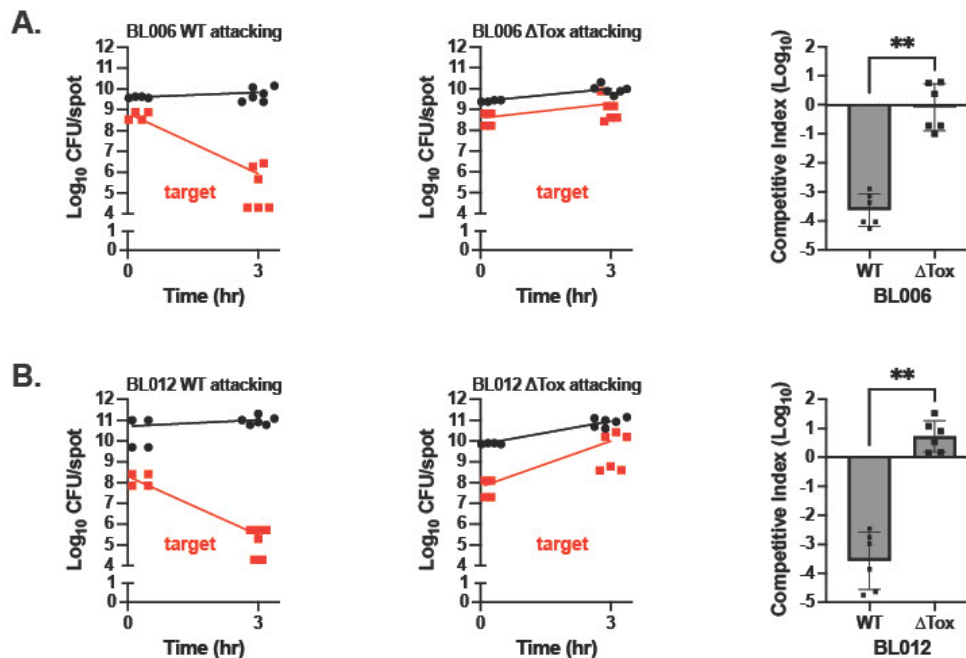
### RESULTS

#### **Variation in *P. aeruginosa* CDI.**

From prior studies, we know that *P. aeruginosa* strain BL017 strongly inhibits an isogenic mutant with a deletion in the *cdiA*-toxin domain and *cdiI* immunity gene ( $\Delta$ ToxIm) [33]. To investigate the inhibitory capacity of other *cdiA* alleles, we generated a panel of 13 additional  $\Delta$ ToxIm target strains representing 5 toxin alleles (Fig. 2, Table 5). Target strains were marked with a gentamicin resistance cassette at the neutral *attTn7* site in the chromosome to differentiate them from attacking strains. Competition assays were performed on solid media to measure the WT strain's ability to inhibit the replication of its respective target strain. To determine if any observed inhibition was imparted by CdiA,  $\Delta$ ToxIm strains without a gentamicin resistance marker were used as attackers against the same marked target strain.

The first group of strains we studied share CdiA toxin domain 3 (Tox3) (Fig. 3). Strains BL006, BL53, BL063, and BL083 are part of a globally distributed clonal complex 446 [36] while BL012 is a phylogenetically distinct isolate encoding the same *cdiA*<sup>Tox3</sup> allele (Fig. 2). Regardless of the strain background, WT attacking strains strongly inhibited their respective target strain (Fig. 3). We observed a 10- to 1,000-fold reduction in the target cell population over the 3-hour competition. In contrast,  $\Delta$ ToxIm attacking strains were unable to inhibit target cell growth suggesting that the observed inhibition imparted by WT strains is through CdiA. A competitive index (CI) was calculated from the enumerated bacteria to quantify the relative fitness of the target

cell population in competition with the different attacking strains. The CI is simply a ratio of the target cells to the attacking cells at output divided by the same input ratio (see methods). A CI equal to 1 indicates the target to attacking ratio did not change over the incubation period; in other words, the target can fully compete with the attacker. However, as the CI decreases below 1, the target-to-attacking ratio at output is less than input, indicating that the target population cannot compete with the attackers. We observed a significant difference in CI comparing WT to  $\Delta$ ToxIm attacking cells for the strains we selected (Fig. 3). Thus, *P. aeruginosa* strains that encode for the Tox3 *cdiA* allele all strongly perform CDI. Though the activity of Tox3 has never been experimentally determined, it is predicted to have nucleic acid deaminase activity and can be structurally modeled after nucleotide deaminases from other bacteria (Fig. 4).



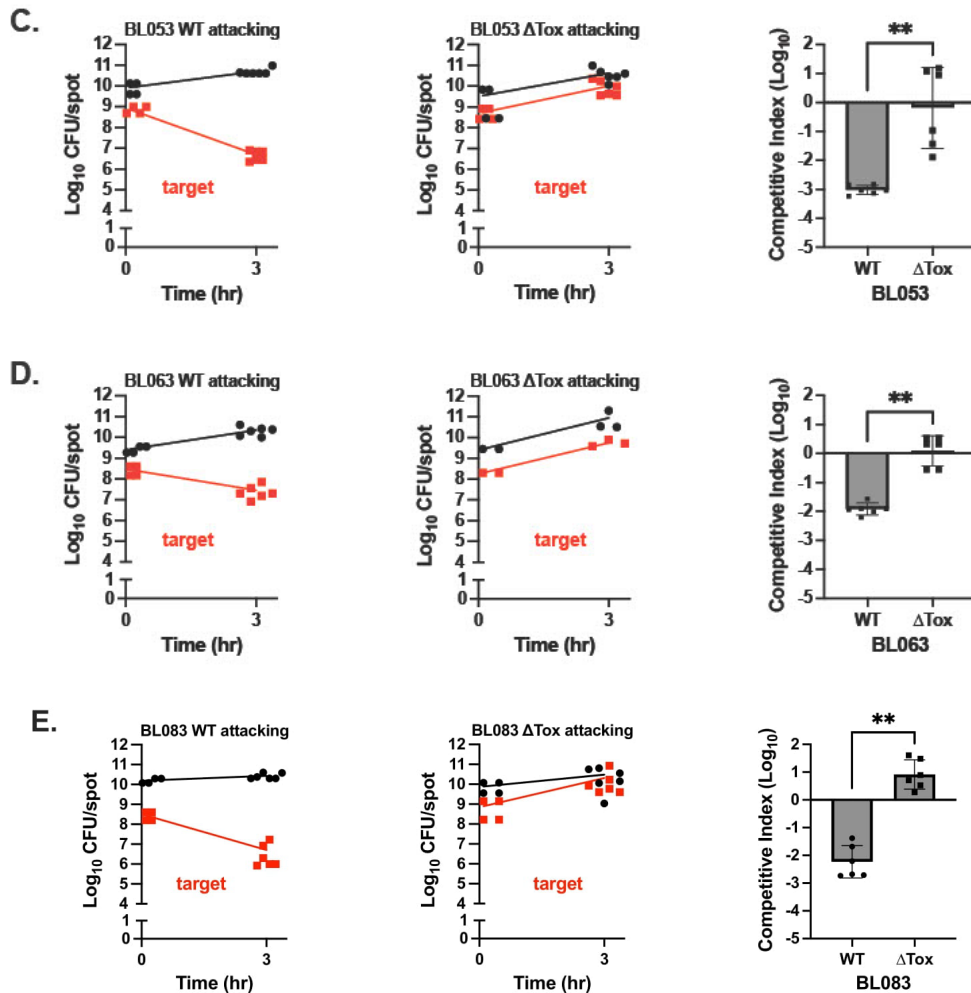


**Figure 3. *P. aeruginosa* Strains with CdiA-Tox3 Perform CDI under Standard Conditions.** Competition assays were performed with *P. aeruginosa* strains BL006 (A), BL012 (B), BL053 (C), BL063 (D), and BL083 (E). For all competitions, target strains are mutants containing a deletion of the *cdiA* toxin domain and cognate *cdiI* immunity gene in the respective parental strain background (*cdiAΔtoxΔcdiI*). Attacking strains are either the wild-type (WT) parental strain (left graph) or CdiA toxin deletion ( $\Delta$ Tox) strain (middle graph). Attacking and target strains were concentrated, mixed at a 10:1 ratio respectively, and spotted on an LB plate to promote interbacterial competition. A separate aliquot of the input mixture was used to enumerate input attacking (black symbols) and target (red symbols) colony forming units (CFU). Competition spots were harvested after 3 hr for output bacterial enumeration. A competitive index (right graph) was calculated to determine the relative fitness of the target strain against WT or  $\Delta$ Tox attacking strains. The  $\text{Log}_{10}$  transformed competitive index data is plotted; a value  $< 0$  indicates the target could not compete with the attacking strain. Individual data points are plotted as well as the mean  $\pm$  SD (Mann-Whitney test, \*\* $P < 0.01$ , \*\*\* $P < 0.001$ , ns = not significant).

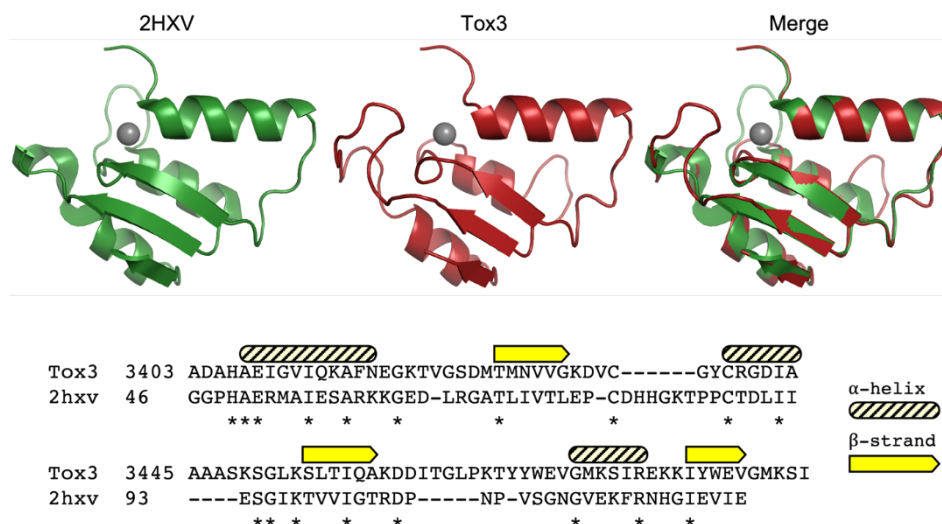


**Figure 4. The CdiA-Tox3 Domain Is Predicted to Have Nucleotide Deaminase Activity.** Swiss-model [35] was used to predict the structure and function of the CdiA-Tox3 domain. The structure with the highest modeling score resembles a cytidine deaminase domain from protein TM1828 of *Thermotoga maritima* (PDB: 2hxv). The known structure of TM1828 cytidine deaminase domain (A), predicted structure of CdiA-Tox3 (B), and an overlay of the two structures (C) are depicted with a coordinating zinc ion (grey). (D) An amino acid alignment from the Tox3 Swiss-model prediction highlights conserved residues and secondary structures.

The next group of strains we studied share the CdiA toxin domain 5 (Tox5) (Figure 5). As with the Tox 3 strains, we chose the phylogenetically distinct strains BL002 and BL017 to investigate Tox5 (Fig. 2). Both strains strongly inhibited their respective targets (Fig 5). We observed a 1000-fold reduction of the target cell population over a 3-hour competition. As with the Tox3 strains, the  $\Delta$ ToxIm mutants were unable to inhibit the target cell population suggesting the observed inhibition was imparted by CdiA. The structure of the CdiA-Tox5 domain has been solved and was experimentally determined to have tRNase activity against Gln and Ala tRNA molecules [33].

Coincidentally, structural prediction of the CdiA-Tox11 domain resulted in a model that resembles the Tox5 domain as well as the toxin domain from colicin D, another known tRNase involved in bacterial competition (Fig. 7). As with the Tox5 strains, competition with the Tox11

strain BL023 resulted in a 1000-fold decrease of the target cell population after 3 hours (Fig. 6). By overlaying the structures of the colicin D, Tox11, and Tox5 toxin domains, we observed that all 3 toxins share a conserved histidine residue that is known to have catalytic activity for ColD and Tox5 (Fig. 7D, inset) [33]. Thus, although the primary sequence of these different domains largely differs, the tRNase structure with catalytic histidine residue appears conserved. Moreover, tRNase toxin domains appear to be potent effectors of interbacterial competition.

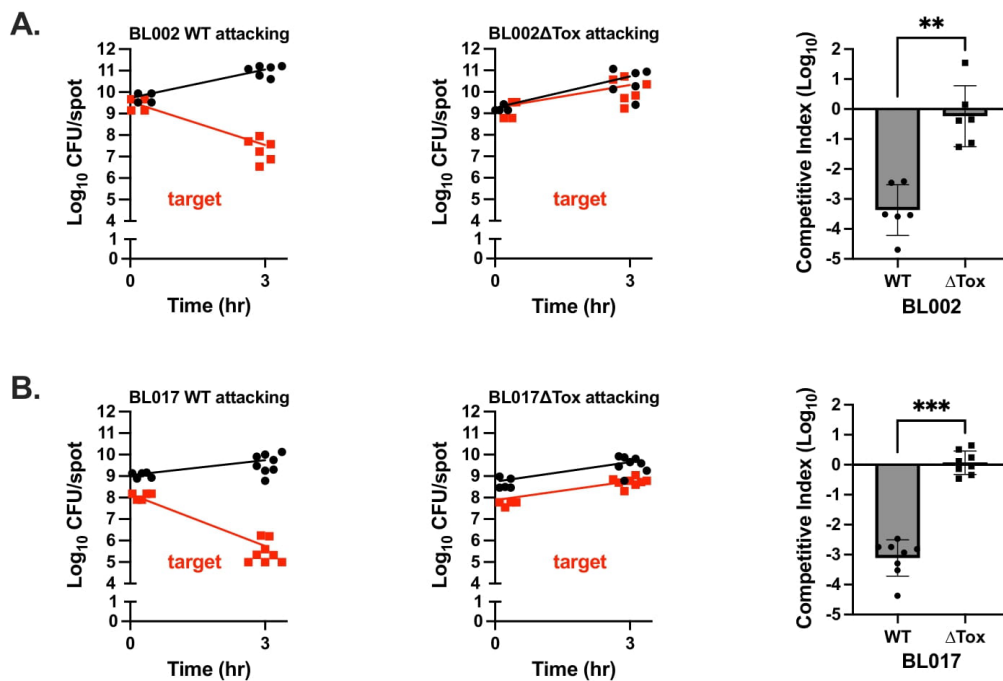


**Figure 5. *P. aeruginosa* Strains with CdiA-Tox5 Perform CDI under Standard Conditions.** Competition assays were performed with *P. aeruginosa* strains BL002 (A), BL017 (B) as described in figure 2. CI data points are plotted as well as the mean  $\pm$  SD (Mann-Whitney test, \*\* $P < 0.01$ , \*\*\* $P < 0.001$ , ns = not significant).

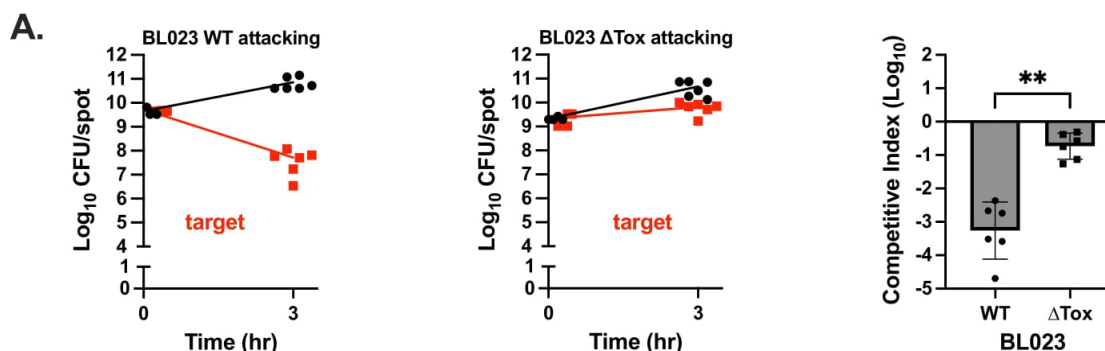


**Figure 6. *P. Aeruginosa* Strains with CdiA-Tox11 Perform CDI under Standard Conditions.**

Competition assays were performed with *P. aeruginosa* strain BL023 as described in figure 2. CI data points are plotted as well as the mean  $\pm$  SD (Mann-Whitney test, \*\* $P < 0.01$ , \*\*\* $P < 0.001$ , ns = not significant).

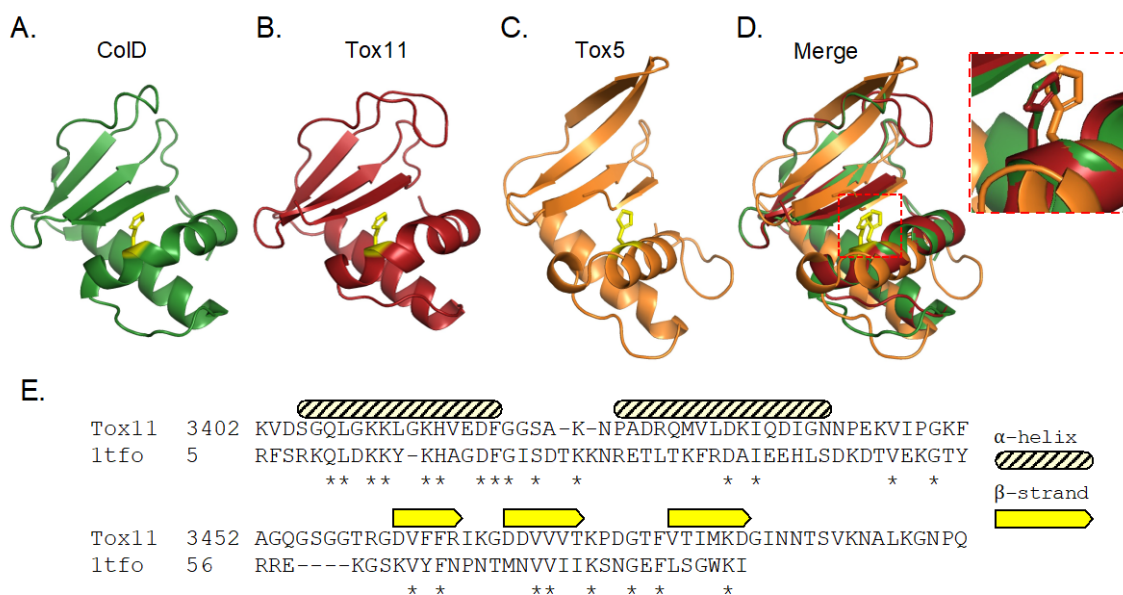


**Figure 7. The CdiA-Tox11 Domain Is Predicted to Have tRNase Activity.** Swiss-model [35] was used to predict the structure and function of the CdiA-Tox11 domain. The structure with the highest modeling score resembles the Colicin D toxin domain (PDB: 1tfo), a known tRNase [37]. The known structure of ColicinD toxin domain (A), predicted structure of CdiA-Tox11 (B), known structure of CdiA-Tox5, and an overlay of the three structures (C) are depicted. (D) Inset image highlights the shared catalytic His residue. (E) An amino acid alignment of ColD and Tox11 highlights conserved residues and predicted secondary structures.

The next group of strains we studied share the CdiA toxin domain 12 (Tox12) (Figure 8). As with our other toxin groups, we chose to investigate strains BL046, BL015 and BL028 because they are phylogenetically distinct (Figure 2). Unlike our observations with Tox3, Tox5, and Tox 11 containing strains, none of the strains encoding the Tox12 *cdiA* allele domain displayed a strong inhibition of their respective target strains (Fig. 8). The Competition Index of Tox12 containing strains are below our cutoff of -2 which indicates 100-fold reduction. Since we did not observe dramatic reduction of target cell, we couldn't tell whether Tox12 is bactericidal or bacteriostatic. Our prediction is that CdiA toxin domain display a gradient of inhibitory phenotype. Strains like BL046 can compete but the competition is not as strong. We were unable to get a predicted structure from SWISS MODEL, but comparison of the Tox12 amino acid sequence to the conserved domain database [38] suggests that it may have some type of RNase activity.

Last, we studied 3 strains that share CdiA toxin domain 10 (Tox10) (Figure 9). We observed that BL040 and BL082 performed strong competition but BL022 performed weak competition. The target cell population of BL040 and BL082 reduced 10- to 1000-fold over 3-hour competition but the target cell population of BL022 increased by about 10-fold after 3 hour (Figure 9). All 3 strains we studied share Tox10 which is predicted to have endonuclease activity (Figure 10), therefore we would expect them to display the same phenotype because nuclease tend to impart strong inhibition. We hypothesized the BL022 may have a physical barrier which limits the toxin delivery, or it cannot be intoxicated by CDI because of mutation in *cdi* locus.



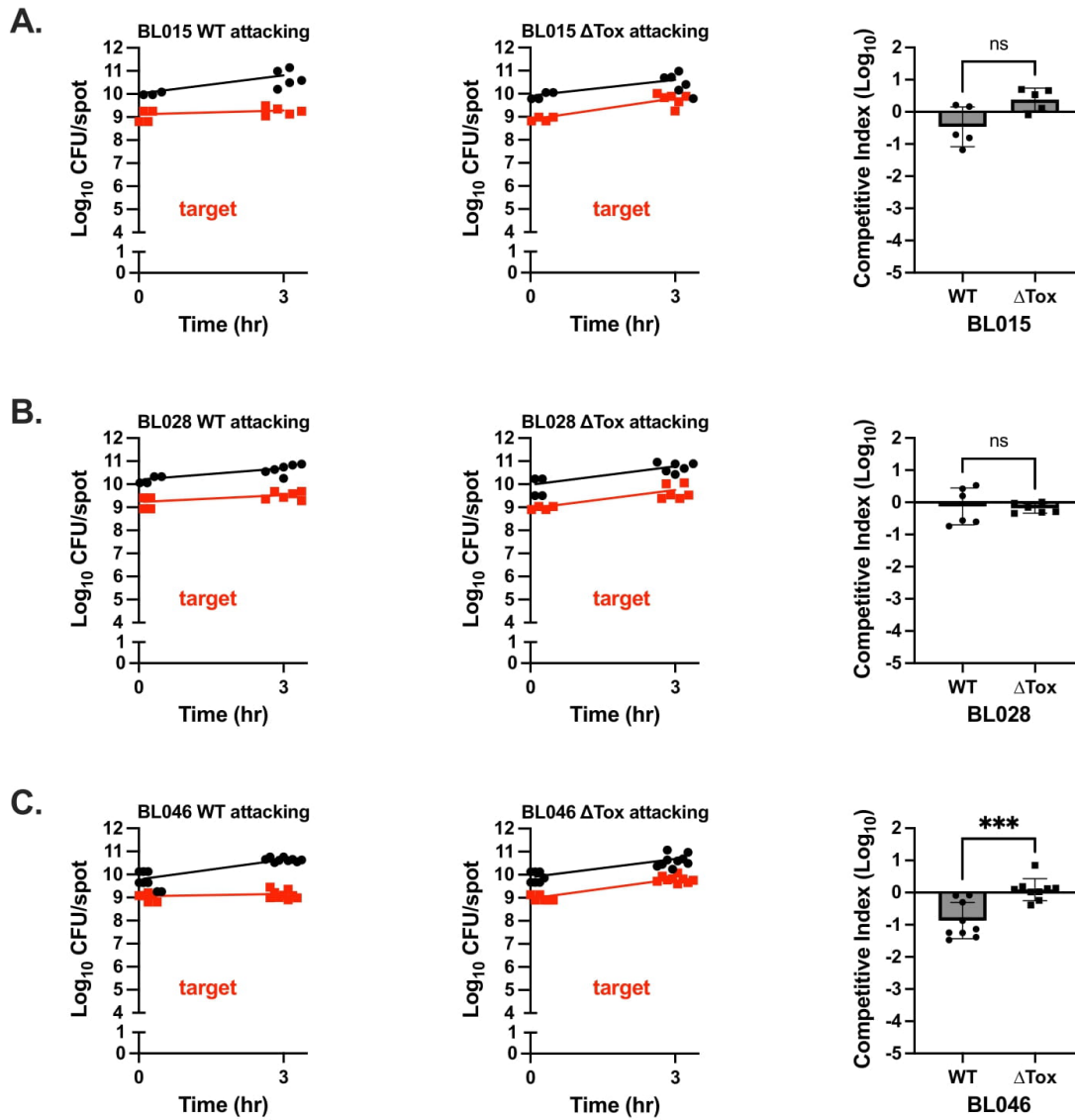


**Figure 8. *P. aeruginosa* Strains with CdiA-Tox12 Do Not Perform CDI under Standard Conditions.** Competition assays were performed with *P. aeruginosa* strains BL015 (A), BL028 (B), and BL046 (C) as described in figure 2. CI data points are plotted as well as the mean  $\pm$  SD (Mann-Whitney test, \*\*P < 0.01, \*\*\*P < 0.001, ns = not significant).

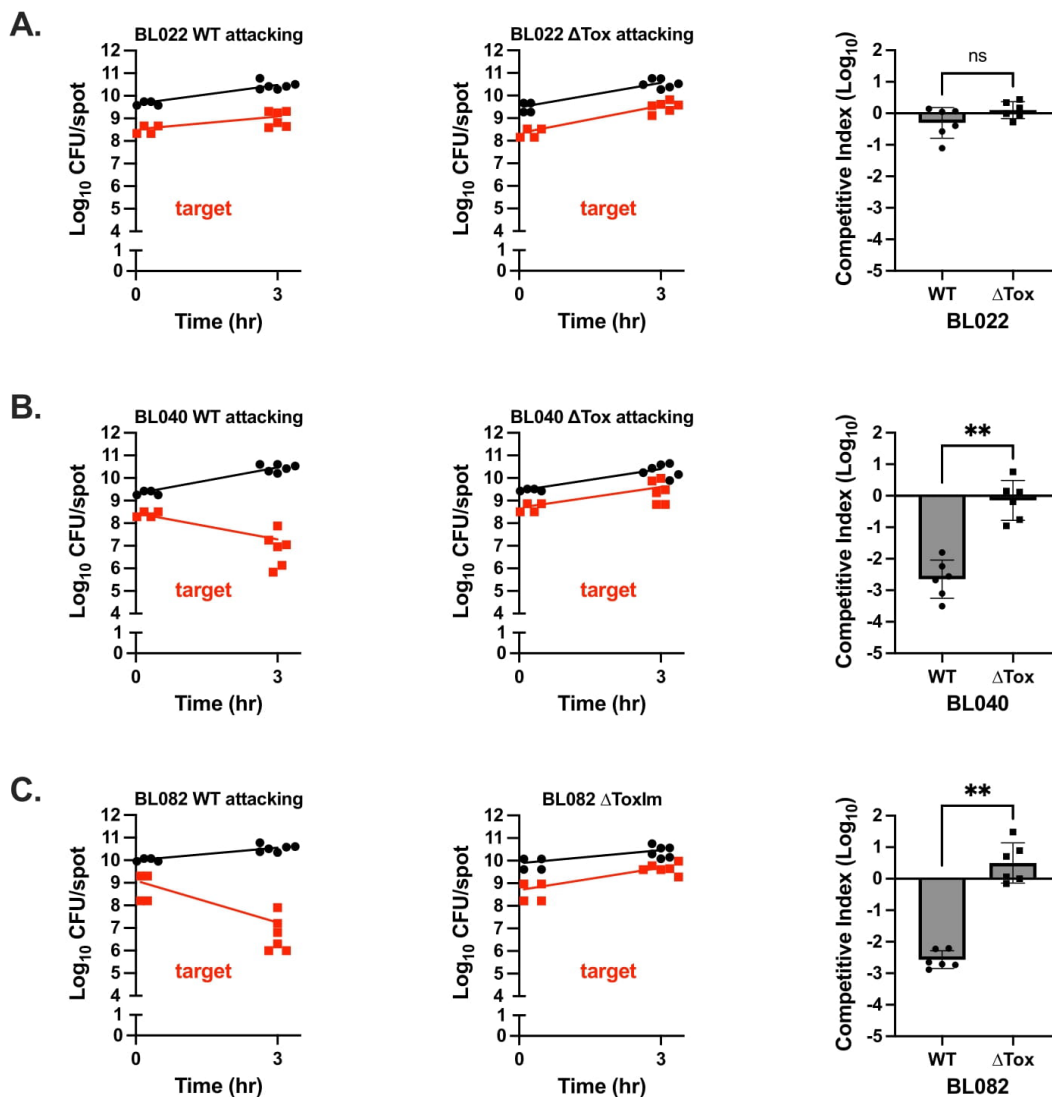


**Figure 9. *P. Aeruginosa* Strains with CdiA-Tox10 Display Variable Competition Phenotypes.** Competition assays were performed with *P. aeruginosa* strains BL022 (A), BL040 (B), and BL082 (C) as described in figure 2. CI data points are plotted as well as the mean  $\pm$  SD (Mann-Whitney test, \*\*P < 0.01, \*\*\*P < 0.001, ns = not significant).

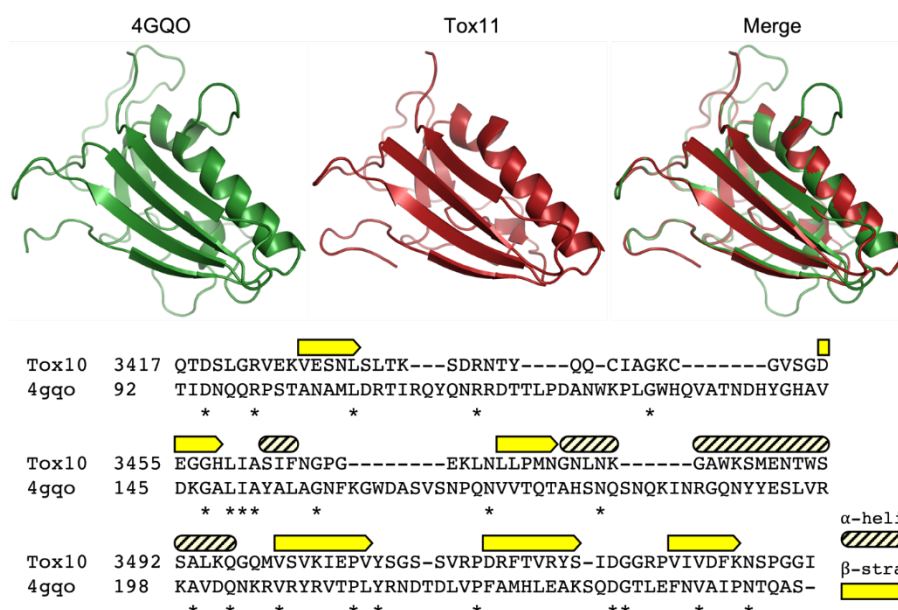


**Figure 10. The CdiA-Tox10 Domain Is Predicted to Have Endonuclease Activity.** Swiss-model [35] was used to predict the structure and function of the CdiA-Tox10 domain. The structure with the highest modeling score resembles NucA from *Streptococcus agalactiae* (PDB: 4gqo), a known endonuclease [39]. The known structure of NucA (A), predicted structure of CdiA-Tox10 (B), and an overlay of the two structures (C) are depicted. (D) An amino acid alignment from the Tox10 Swiss-model prediction highlights conserved residues and secondary structures.

**Table 5. Competition Assay Summary**

Toxin	Predicted Function <sup>a</sup>	Strain	CDI <sup>b</sup>	Group <sup>c</sup>
Tox3	nucleic deaminase acid	BL006	Strong	I
		BL012	Strong	
		BL053	Strong	
		BL063	Strong	
		BL083	Strong	
Tox5	tRNase	BL002	Strong	I
		BL017	Strong	
Tox11	tRNase	BL023	Strong	I
Tox12	RNase?	BL015	Weak	II
		BL028	Weak	
		BL046	Weak	
Tox10	endonuclease	BL022	Weak	III
		BL040	Strong	
		BL082	Strong	

<sup>a</sup>Based upon SWISS-MODEL analysis and Conserved Domain Database search.

<sup>b</sup>“Strong” is defined as an average competitive index  $< 10^{-1}$ . All others are “Weak”.

<sup>c</sup>Groups are based on CDI phenotype within a toxin class as defined in the main text

### **CdiA-Toxin Domains May Differ in Potency.**

Based upon the results of the competition data, we sorted the *P. aeruginosa* strains into three different groups: Group I, all strong competitors within a toxin class; Group II, all weak competitors within a toxin class; Group III, mixed competitors within a toxin class (i.e., some weak and some strong competitors) (Table 5). We first sought to elucidate the difference between group I (strong) and group II (weak) competitors. Our initial hypothesis was that group I strains have higher *cdiA* expression than group II strains. To test this hypothesis, we analyzed *cdiA* transcript levels using RTqPCR. We first compared *cdiA* expression in BL046 (Tox 12, Group II) to BL017 (Tox 5, Group I) and BL063 (Tox 3, Group I) (Fig. 11A). BL046 had a slight but not significant decrease in *cdiA* expression compared to BL017 and a significant decrease compared to BL063. When comparing the results of the competition assays for these 3 strains, it was unclear whether this small amount of transcriptional variation could explain the competitive differences between group I and group II strains (Figs. 3, 5, 8). Furthermore, BL063 had a slightly higher level of expression than BL017 (Fig. 11A) with no concomitant increase in competition (Fig. 3D). To understand the natural variation in *cdiA* expression, we performed RTqPCR on additional Tox12 (group II) and Tox 5 (group I) strains (Fig. 11B, C). We observed slight but non-significant differences in *cdiA* expression in the Tox 12 (group II) strains (Fig. 11B); however, when comparing the Tox 5 (group I) strains, BL002 had a significantly reduced transcript level relative to BL017 (Fig. 11C). This difference was greater than the difference observed between BL046 and BL017 (Fig. 11A). Nonetheless, BL002 is a strong competitor (Fig. 5B). Thus, the natural variation in *cdiA* expression between strains does not explain the different CDI phenotypes. It should be acknowledged that while there are no substantial differences in transcript levels between group I and group II strains, there could be a difference in the amount of CdiA protein displayed at the cell

surface. We are currently developing protocols to directly measure CdiA protein levels but are currently not able to directly address this possibility.

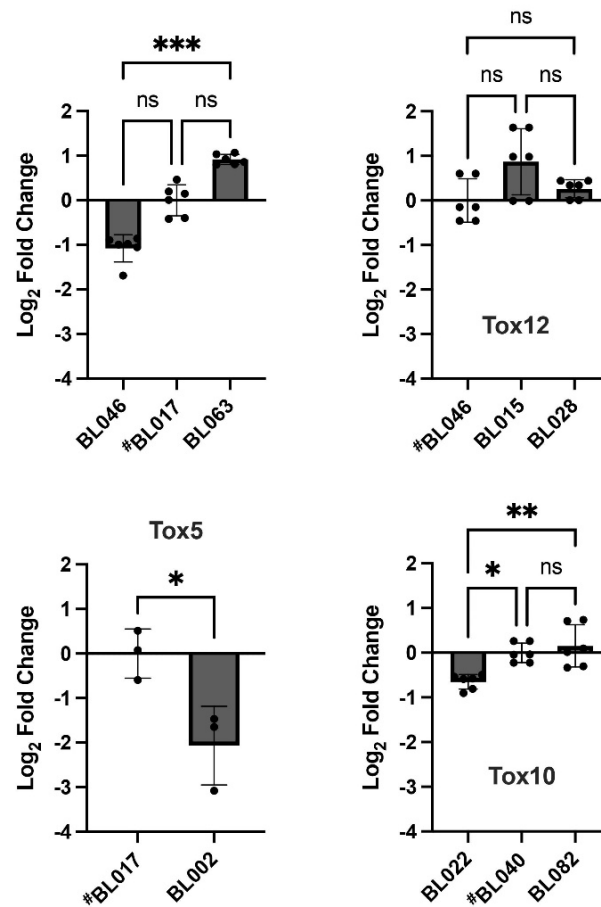


**Figure 11. Expression of *cdiA* Does Not Explain Competition Phenotypes.** Reverse transcription quantitative PCR (RTqPCR) was used to assess *cdiA* expression using the relative quantitation method of Livak and Schmittgen [34]. (A) Expression in the poor competitive strain BL046 was compared to the strong competitive strains BL017 and BL063. Expression was also assessed across different strains within the same toxin class for Tox12 (B), Tox5 (C), and Tox10 (D). Data are represented as Log<sub>2</sub> fold change relative to a control strain marked with the # symbol. Individual data points are provided along with means and standard deviations (Kruskal-Wallis test with Dunn's multiple comparisons, \*\*\* $P < 0.001$ , \*\* $P < 0.01$ , \* $P < 0.05$ , ns = not significant)

An alternative hypothesis to the difference between group I and group II competitors is that the toxin domain from group I strains is more potent than group II strains; in other words, the toxin

domain imparts a stronger inhibition because of its mode of action. Differences in toxin potency have been directly observed in *E. coli* [29]. We initially tried to test this hypothesis by generating CdiA-toxin chimeras. Our goal was to genetically exchange the toxin domain from BL046 (group II) with that of BL017 (group I) and determine whether this increased the competitiveness of BL046 in our assay. Unfortunately, we were unable to obtain a construct that sequenced correctly to use in our competitions. As an alternate approach, we decided to express the CdiA-toxin domain alone or with its cognate immunity factor under the control of an arabinose-inducible promoter in *E. coli*. If the group I toxin domain from BL017 is more potent than the group II toxin domain from BL046, then we would observe a more severe growth inhibition following induction respectively. Moreover, co-expression of the cognate immunity factor should restore bacterial growth. We were unable to obtain constructs that sequenced correctly in the absence of the respective immunity factor, suggesting that the CdiA-toxin domains from BL17 and BL046 are inherently toxic to *E. coli*. However, even when expressed with its respective immunity factor, the BL017 CdiA-toxin domain resulted in a titratable retardation of the *E. coli* growth curve compared to uninduced conditions (Fig. 13A). This same effect was not observed for the BL046 CdiA-toxin domain. To ensure this difference was not attributable to differences in toxin production, cell lysates were collected at 240 minutes post-induction (0.1 mM arabinose, normalized to the same absorbance) and processed for SDS-PAGE and western blot. We observed CdiA-toxin production for both BL046 and BL017 (Fig. 13B), with a slightly stronger band for the BL046 CdiA-toxin, suggesting that the observed growth difference upon induction is not attributable to differences in protein production.

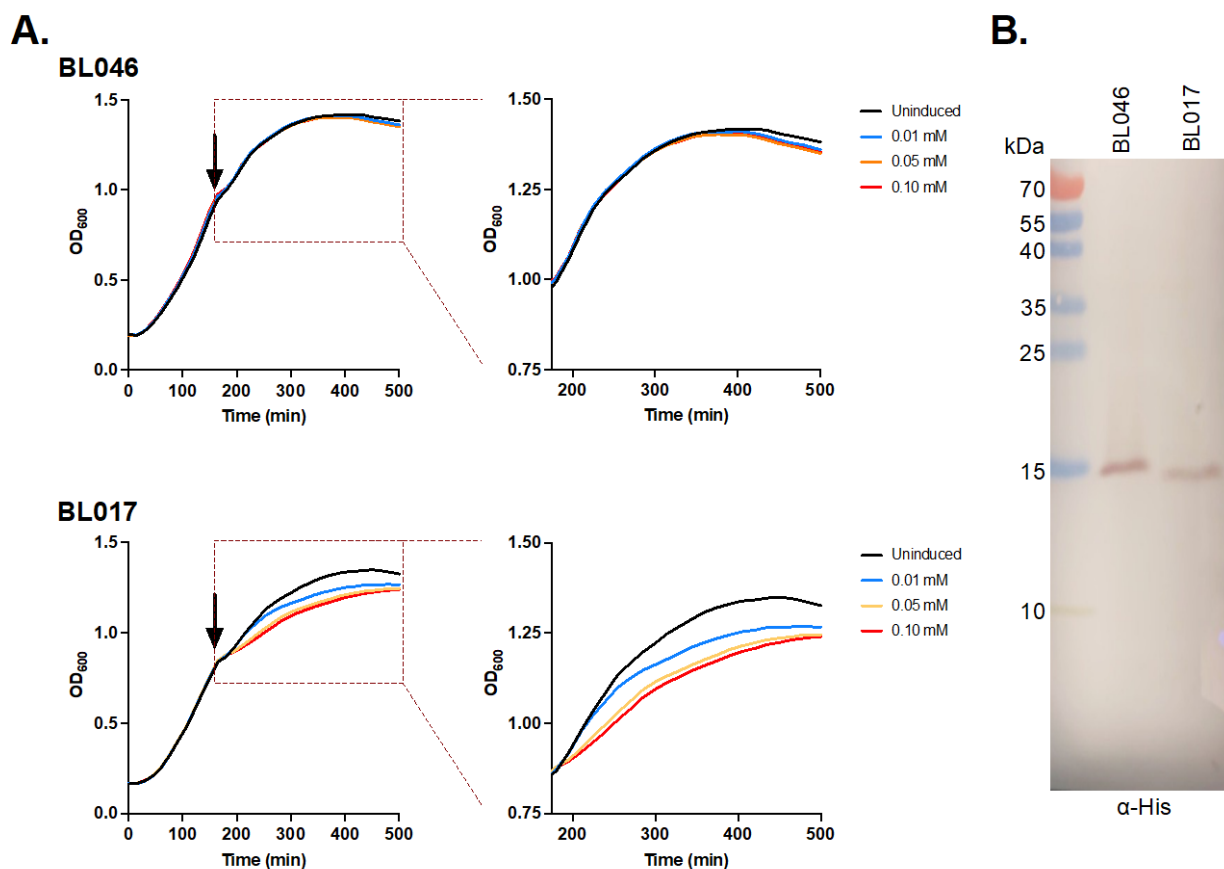


**Figure 12. Heterologous CdiA<sup>BL017</sup> Toxin Expression but Not CdiA<sup>BL046</sup> Toxin Slows Bacteria Growth.** (A) Expression of *cdiA*-Tox and *cdiI* from BL046 (Top) or BL017 (Bottom) in *E. coli* was induced at 180 min (black arrow) with increasing concentrations of IPTG. Bacterial cell growth was monitored by measuring the culture optical density at 600 nm (OD600) over time. Right graphs are a focused subset of the data after induction. (B) Western blot analysis of 0.1 mM induced cell lysates collected at 420 minutes. Membranes were probed with an anti-6xHis primary antibody to detect CdiA toxin production.

As stated above, our inability to clone the Tox12 domain in the absence of the cognate immunity factor suggests that this domain has the potential to antagonize bacterial cell replication, although less than more potent toxins domains (e.g., Tox 5). While under natural laboratory conditions we observe no substantial difference in *cdiA* expression (Fig. 11), we hypothesized that dramatic overexpression of *cdiA* might result in a measurable competition phenotype for BL046. From other's work in the lab, we know that overexpression of the *cdi* locus using the strong pTRC

promoter increases the amount of detectable CdiA on the bacterial surface and significantly enhances CdiA-dependent phenotypes in strain BL017 (unpublished data). Therefore, we exchanged the native *cdi* promoter with the pTRC promoter and tested this strain in competition assays. Where BL046 WT displayed negligible inhibition of a susceptible target strain, the *cdi* overexpression strain strongly inhibited the competing target (Fig. 14). Thus, overexpression of the *cdi* locus does allow for a previously non-competitive strain to strongly perform CDI. We assume that this is because of an overproduction of CdiA resulting in increased delivery of the CdiA-Tox domain into susceptible target cells. Future experiments must be performed to test this assumption. Overall, these data support the hypothesis that there may be potency differences

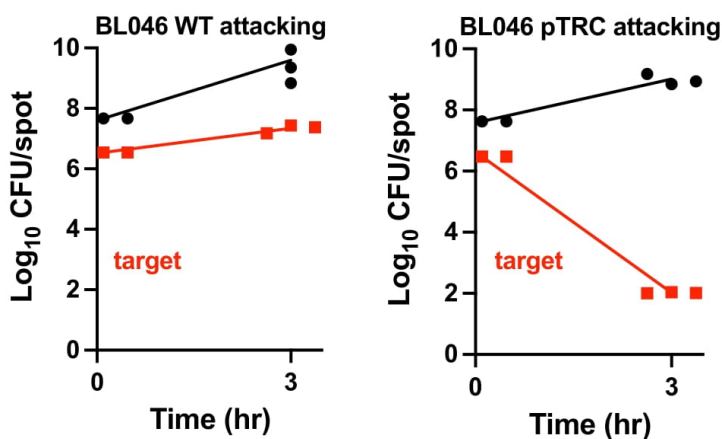


**Figure 13. Overexpression of the *cdi* Locus in BL046 Promotes CDI.** Competition assays were performed as described in figure 2 with *P. aeruginosa* attacking strains BL046 WT (left) or BL046 engineered to overexpress the *cdi* locus (BL046 pTRC, right).



### Strain BL022 Is Susceptible to CDI but Does Not Produce a Functional CdiA

We next sought to understand the competitive differences within group III strains containing CdiA-toxin 10 (Table 5). Specifically, why do BL40 and BL82 have strong competition phenotypes but BL022 displays a weak phenotype (Fig. 9)? As with group I and group II strains, we asked whether *cdiA* expression was different between the group III strains. BL022 had a very modest but significant reduction in *cdiA* expression compared to the other group III strains (Fig. 11D); however, the slightly reduced expression in BL022 falls within the natural variation observed across all *P. aeruginosa* strains. Therefore, the variance in *cdiA* expression between group III strains does not necessarily explain the different CDI phenotypes (Fig. 9).

It was recently observed that overproduction of a polysaccharide capsule can protect *Acinetobacter baumannii* from CDI [41]. In this context, it is believed that the excess capsule acts as a physical barrier preventing close contact between bacterial cells. Some *P. aeruginosa* clinical isolates are known to overproduce extracellular polysaccharides such as alginate, especially when isolated from the sputum of patients with cystic fibrosis [40]. Moreover, excess *P. aeruginosa* alginate production can disrupt interbacterial interactions with *Staphylococcus aureus* [42]. Although BL022 does not display the traditional mucoid phenotype associated with alginate overproduction, we hypothesized that BL022 could be inherently resistant to CDI because it limits physical contact with other bacterial cells by some other means. If this were true, then BL022 should be resistant to CDI from a different attacking strain as well. *P. aeruginosa* strain BL040 encodes the same *cdiA* allele (Table 5) but is a strong competitor against an isogenic CdiAΔToxIM strain (Fig. 9B). When BL040 was used as an attacking strain in competition with WT BL022 as a target strain, we observed no competitive defect for BL022 (Fig. 14C). However, when BL040

was used as an attacking strain in competition with a BL022 *CdiA*Δ*ToxIm* strain, there was a dramatic reduction (>2-log) in target CFU over 3 hr (Fig. 12D). This data suggests two major points: (1) BL022 must not limit interbacterial contact in a way that would disrupt CDI; (2) WT BL022 produces a functional CdiI immunity factor. When we also consider that there was no substantial reduction in *cdiA* expression for BL022 compared to BL040, a likely interpretation is that the *cdiA* gene in BL022 must have a mutation that translates a non-functional CdiA protein. When BL022 was used as an attacking strain in competition with WT BL040 as a target strain, we observed competitive defect for BL040. When BL022 was used as an attacking strain in competition with BL040 *CdiA*Δ*ToxIm*, the same competitive defect was observed with no additional growth defect. Therefore, we think BL022 must inhibit BL040 through another mechanism and the result is not shown here. -The genome of BL022 is currently in a draft format with the *cdiA* gene incompletely assembled over multiple contigs. Current efforts are underway to obtain a BL022 finished genome so that we can investigate this possibility.

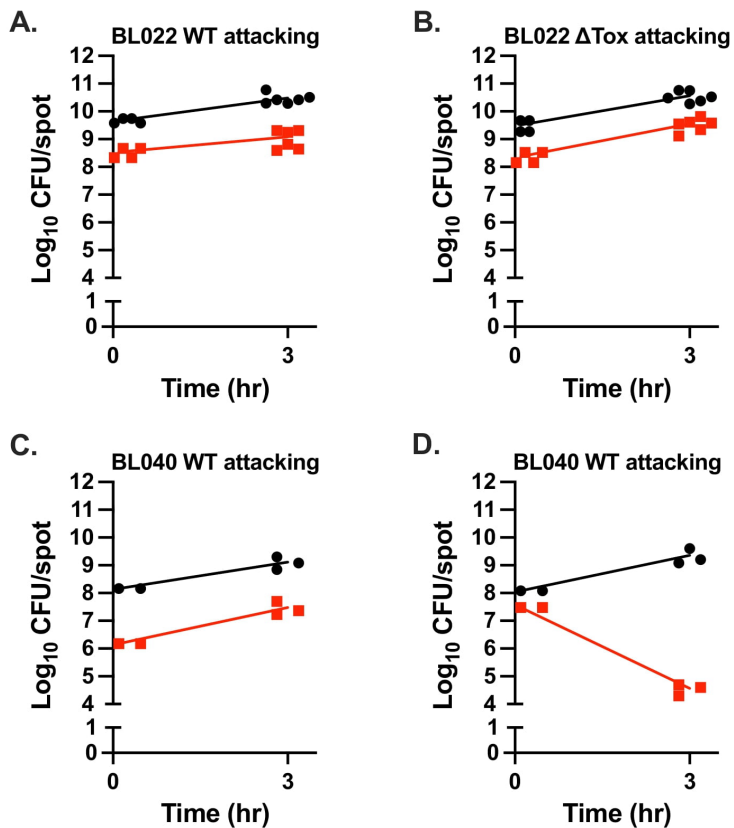


**Figure 14. BL022 Is Susceptible to CDI by a Different Strain with the Same Tox10 Domain.** Competition assays were performed using attacking strains BL022 WT (A), BL022  $\Delta$ Tox (B), and BL040 WT (C, D) as described in figure 2. BL022 $\Delta$ ToxIm was used as the target strain for A, B, and D. BL022 WT was used as the target strain for C. Panels A and B are replicated from figure 9A for ease of reference.

## CHAPTER FOUR

### DISCUSSION

Bioinformatics revealed that *P. aeruginosa* strains encode a pool of diverse *cdiA* alleles[1]. We examined the CDI strength of *P. aeruginosa* biological isolates through competing the WT strain against the  $\Delta$ ToxImm target on solid surfaces. We observed that some strains were able to perform strong competition while some were only able perform weak competition. In general, strains with the same *cdiA* allele impart the same level of growth inhibition to their respective target strains. Although some *P. aeruginosa* biological isolates that possess the same *cdiA* alleles are phylogenetically distinct, they did not show difference in CDI mediated growth inhibition. We only identified one strain, BL022, which behaves differently compared to the strains that share the same CDI with it. In this case, BL022 is susceptible to CDI intoxication but is unable to produce a functional CdiA protein to intoxicate target cells. We hypothesize that the toxin domain produced by BL022 has frameshift mutation that might arise during horizontal gene transfer. Because the *cdiA* gene fragment is too large and has many repetitive regions, we were not able to fully sequence *cdiA* gene for BL022. Besides BL022, we also found that strains with Tox12 background mediate weak competition. We do not know the benefit of producing a less potent toxin within a mixed community. Some research showed that *P. aeruginosa* is more virulent when co-cultured with other bacterial species such as *Staphylococcus aureus*. Co-culture also changes the community structure within a biofilm and enhances the antibiotics resistance of 2 species [10].

Weak competitors may form a symbiotic relationship with other species to persist during an infection.

We hypothesized that the differences we observed in competition is due to variation in gene expression, difference in protein potency or the combination of both. Quantitative RT-PCR result showed that transcript level varied slightly among strains, but the transcriptional variation could not explain the difference we observed in competition because some weak competitors also had a relatively high transcript level. Although different toxins have different activity, the absolute expression informed us that potent proteins do not always have lower expression. We originally expected proteins with high potency, such as Tox5, have lower gene expression and the proteins with low potency have higher gene expression. Our result showed that *cdiA* expression varies within strains that share the same *cdi* background. In the later experiment in which we overexpressed *cdi* locus in BL046, we demonstrated that increasing the expression of *cdi* could make a non-competitive strain to perform strong CDI.

Next, we tried to measure the protein potency by constructing CdiA chimeras and measuring CdiA potency in a reporter strain. Our initial approach was to construct a chimera that exchanges the toxin domain of BL046 with the toxin domain of BL017 and measure the competitiveness of BL046. However, the chimera we generated had frameshift mutation or reverted to wild-type. It was technically difficult to generate a *cdiA* chimera because it contains many repetitive regions. In our alternative approach we co-expressed CdiA-CT/CdiI of BL017 and BL046 in *E. coli*. The goal is to measure *E. coli* growth attenuation upon toxin production. BL017 toxin domain resulted in a titratable slowing of growth curve but the same effect was not observed with BL046 toxin domain. Although the immunity factor neutralizes partial toxin domain under induction, we were still able to see the difference in protein potency through *E. coli* growth

attenuation. This experiment was done once, and each experimental condition was performed in triplicates. This result suggested that different CdiA-CT vary in their protein potency. A strong competitor encodes *cdiA*-CT that is more potent than that of a weak competitor. The variation in the CdiA-CT potency contributes to the differences we observed in competition rather than gene expression. Previous research showed that *P. aeruginosa cdiA*- toxin domains are highly diverse using genomic analysis, but no research has studied whether CdiA-CT diversity would impact growth inhibition. Here we showed that *P. aeruginosa* that encodes different CdiA vary in the ability to perform CDI. Strains encode Tox 3, Tox 5, Tox 10 and Tox11 imparted strong inhibition to their target strains while Tox 12 imparted weak inhibition to their target strains. Our data supported that protein potency plays an important role in CDI-mediated growth inhibition. Future research on CDI can focus on protein potency and the delivery of the toxin domain. So far, we managed to clone the toxin domain with the immunity factor into a construct, but we were unable to obtain a correct construct without the respective immunity factor. To characterize the potency of toxin domains, we should develop a tool that allows us to study the toxin domain alone. Alongside, future study can also try to construct chimeras which swap the toxin domains and immunity factors among strong competitors and weak competitors. Besides protein potency, there may be other factors that affect CDI intoxication. We cannot conclude that the difference in competition is only affected by variation in protein potency.

*P.aeruginosa* is a common contaminant in the clinical setting that contaminate either medical device or the water source of a hospital, leading to infections in patients. We purpose that CDI can be used as a strategy to treat hospital water contamination. Because CDI target non-siblings, we can potentially engineer a strain that encodes potent toxins and eradicate *P.aeruginosa* that contaminate the water source with this engineered strain. *P. aeruginosa* is resistant to many

antibiotics which result difficulties treating contamination. The advantage of treating contamination with CDI is that CDI deliver toxin domain directly to target cells through T5SS. Even antibiotic-resistant strains can be subject to CDI intoxication.

## REFERENCE LIST

- [1] Allen, J. P., & Hauser, A. R. (2019). Diversity of Contact-Dependent Growth Inhibition Systems of *Pseudomonas aeruginosa*. *Journal of bacteriology*, 201(14), e00776-18. <https://doi.org/10.1128/JB.00776-18>
- [2] Aoki SK, Pamma R, Hernday AD, Bickham JE, Braaten BA, Low DA. Contact-dependent inhibition of growth in *Escherichia coli*. *Science*. 2005 Aug 19;309(5738):1245-8. <https://doi:10.1126/science.1115109>. PMID: 16109881.
- [3] Aoki, S. K., Diner, E. J., de Roodenbeke, C. T., Burgess, B. R., Poole, S. J., Braaten, B. A., Jones, A. M., Webb, J. S., Hayes, C. S., Cotter, P. A., & Low, D. A. (2010). A widespread family of polymorphic contact-dependent toxin delivery systems in bacteria. *Nature*, 468(7322), 439–442. <https://doi.org/10.1038/nature09490>
- [4] Poole, S. J., Diner, E. J., Aoki, S. K., Braaten, B. A., t'Kint de Roodenbeke, C., Low, D. A., & Hayes, C. S. (2011). Identification of functional toxin/immunity genes linked to contact-dependent growth inhibition (CDI) and rearrangement hotspot (Rhs) systems. *PLoS genetics*, 7(8), e1002217. <https://doi.org/10.1371/journal.pgen.1002217>
- [5] Wäneskog, M., Halvorsen, T., Filek, K., Xu, F., Hammarlöf, D. L., Hayes, C. S., Braaten, B. A., Low, D. A., Poole, S. J., & Koskiniemi, S. (2021). *Escherichia coli* EC93 deploys two plasmid-encoded class I contact-dependent growth inhibition systems for antagonistic bacterial interactions. *Microbial genomics*, 7(3), mgen000534. <https://doi.org/10.1099/mgen.0.000534>
- [6] Stubbendieck, R. M., & Straight, P. D. (2016). Multifaceted Interfaces of Bacterial Competition. *Journal of bacteriology*, 198(16), 2145–2155. <https://doi.org/10.1128/JB.00275-16>
- [7] Ikryannikova, L. N., Kurbatov, L. K., Gorokhovets, N. V., & Zamyatnin, A. A., Jr (2020). Contact-Dependent Growth Inhibition in Bacteria: Do Not Get Too Close!. *International journal of molecular sciences*, 21(21), 7990. <https://doi.org/10.3390/ijms21217990>
- [8] Weiland-Bräuer N. (2021). Friends or Foes-Microbial Interactions in Nature. *Biology*, 10(6), 496. <https://doi.org/10.3390/biology10060496>
- [9] Timothy A. Klein, Shehryar Ahmad, John C. Whitney. (2020) Contact-Dependent Interbacterial Antagonism Mediated by Protein Secretion Machines. *Trends in Microbiology*, Volume 28, Issue 5, Pages 387-400, ISSN 0966-842X. <https://doi.org/10.1016/j.tim.2020.01.003>
- [10] Sadikot, R. T., Blackwell, T. S., Christman, J. W., & Prince, A. S. (2005). Pathogen-host interactions in *Pseudomonas aeruginosa* pneumonia. *American journal of respiratory and critical care medicine*, 171(11), 1209–1223. <https://doi.org/10.1164/rccm.200408-1044SO>



- [11] Pang, Z., Raudonis, R., Glick, B. R., Lin, T. J., & Cheng, Z. (2019). Antibiotic resistance in *Pseudomonas aeruginosa*: mechanisms and alternative therapeutic strategies. *Biotechnology advances*, 37(1), 177–192. <https://doi.org/10.1016/j.biotechadv.2018.11.013>
- [12] Ruhe, Z. C., Low, D. A., & Hayes, C. S. (2020). Polymorphic Toxins and Their Immunity Proteins: Diversity, Evolution, and Mechanisms of Delivery. *Annual review of microbiology*, 74, 497–520. <https://doi.org/10.1146/annurev-micro-020518-115638>
- [13] Sgro, G. G., Oka, G. U., Souza, D. P., Cenens, W., Bayer-Santos, E., Matsuyama, B. Y., Bueno, N. F., Dos Santos, T. R., Alvarez-Martinez, C. E., Salinas, R. K., & Farah, C. S. (2019). Bacteria-Killing Type IV Secretion Systems. *Frontiers in microbiology*, 10, 1078. <https://doi.org/10.3389/fmicb.2019.01078>
- [14] Coulthurst S. (2019). The Type VI secretion system: a versatile bacterial weapon. *Microbiology (Reading, England)*, 165(5), 503–515. <https://doi.org/10.1099/mic.0.000789>
- [15] Wood, T. E., Howard, S. A., Förster, A., Nolan, L. M., Manoli, E., Bullen, N. P., Yau, H., Hachani, A., Hayward, R. D., Whitney, J. C., Vollmer, W., Freemont, P. S., & Filloux, A. (2019). The *Pseudomonas aeruginosa* T6SS Delivers a Periplasmic Toxin that Disrupts Bacterial Cell Morphology. *Cell reports*, 29(1), 187–201.e7. <https://doi.org/10.1016/j.celrep.2019.08.094>
- [16] Fan, E., Chauhan, N., Udatha, D., Leo, J. C., & Linke, D. (2016). Type V Secretion Systems in Bacteria. *Microbiology spectrum*, 4(1), 10.1128/microbiolspec.VMBF-0009-2015. <https://doi.org/10.1128/microbiolspec.VMBF-0009-2015>
- [17] Ruhe, Z. C., Subramanian, P., Song, K., Nguyen, J. Y., Stevens, T. A., Low, D. A., Jensen, G. J., & Hayes, C. S. (2018). Programmed Secretion Arrest and Receptor-Triggered Toxin Export during Antibacterial Contact-Dependent Growth Inhibition. *Cell*, 175(4), 921–933.e14. <https://doi.org/10.1016/j.cell.2018.10.033>
- [18] Aoki, S. K., Webb, J. S., Braaten, B. A., & Low, D. A. (2009). Contact-dependent growth inhibition causes reversible metabolic downregulation in *Escherichia coli*. *Journal of bacteriology*, 191(6), 1777–1786. <https://doi.org/10.1128/JB.01437-08>
- [19] Willett, J. L., Gucinski, G. C., Fatherree, J. P., Low, D. A., & Hayes, C. S. (2015). Contact-dependent growth inhibition toxins exploit multiple independent cell-entry pathways. *Proceedings of the National Academy of Sciences of the United States of America*, 112(36), 11341–11346. <https://doi.org/10.1073/pnas.1512124112>
- [20] Bartelli, N. L., Sun, S., Gucinski, G. C., Zhou, H., Song, K., Hayes, C. S., & Dahlquist, F. W. (2019). The Cytoplasm-Entry Domain of Antibacterial CdiA Is a Dynamic  $\alpha$ -Helical Bundle with Disulfide-Dependent Structural Features. *Journal of molecular biology*, 431(17), 3203–3216. <https://doi.org/10.1016/j.jmb.2019.05.049>
- [21] Zhang, D., de Souza, R. F., Anantharaman, V., Iyer, L. M., & Aravind, L. (2012). Polymorphic toxin systems: Comprehensive characterization of trafficking modes, processing, mechanisms of action, immunity and ecology using comparative genomics. *Biology direct*, 7, 18. <https://doi.org/10.1186/1745-6150-7-18>
- [22] Iyer, L. M., Burroughs, A. M., Anand, S., de Souza, R. F., & Aravind, L. (2017). Polyvalent Proteins, a Pervasive Theme in the Intergenomic Biological Conflicts of Bacteriophages and

Conjugative Elements. *Journal of bacteriology*, 199(15), e00245-17. <https://doi.org/10.1128/JB.00245-17>

[23] García-Bayona, L., & Comstock, L. E. (2018). Bacterial antagonism in host-associated microbial communities. *Science (New York, N.Y.)*, 361(6408), eaat2456. <https://doi.org/10.1126/science.aat2456>

[24] Hillman, K., & Goodrich-Blair, H. (2016). Are you my symbiont? Microbial polymorphic toxins and antimicrobial compounds as honest signals of beneficial symbiotic defensive traits. *Current opinion in microbiology*, 31, 184–190. <https://doi.org/10.1016/j.mib.2016.04.010>

[25] Makarova, K. S., Wolf, Y. I., Karamycheva, S., Zhang, D., Aravind, L., & Koonin, E. V. (2019). Antimicrobial Peptides, Polymorphic Toxins, and Self-Nonself Recognition Systems in Archaea: an Untapped Armory for Intermicrobial Conflicts. *mBio*, 10(3), e00715-19. <https://doi.org/10.1128/mBio.00715-19>

[26] Ruhe, Z. C., Low, D. A., & Hayes, C. S. (2013). Bacterial contact-dependent growth inhibition. *Trends in microbiology*, 21(5), 230–237. <https://doi.org/10.1016/j.tim.2013.02.003>

[27] Yamashita, K., Mori, A., & Otsuki, S. (1990). Changes in brain thyrotropin-releasing hormone (TRH) of seizure-prone El mice. *Experimental neurology*, 108(1), 71–75. [https://doi.org/10.1016/0014-4886\(90\)90009-h](https://doi.org/10.1016/0014-4886(90)90009-h)

[28] Beck, C. M., Morse, R. P., Cunningham, D. A., Iniguez, A., Low, D. A., Goulding, C. W., & Hayes, C. S. (2014). CdiA from *Enterobacter cloacae* delivers a toxic ribosomal RNase into target bacteria. *Structure (London, England : 1993)*, 22(5), 707–718. <https://doi.org/10.1016/j.str.2014.02.012>

[29] Myers-Morales, T., Oates, A. E., Byrd, M. S., & Garcia, E. C. (2019). Burkholderia cepacia Complex Contact-Dependent Growth Inhibition Systems Mediate Interbacterial Competition. *Journal of bacteriology*, 201(12), e00012-19. <https://doi.org/10.1128/JB.00012-19>

[30] Mercy, C., Ize, B., Salcedo, S. P., de Bentzmann, S., & Bigot, S. (2016). Functional Characterization of *Pseudomonas* Contact Dependent Growth Inhibition (CDI) Systems. *PloS one*, 11(1), e0147435. <https://doi.org/10.1371/journal.pone.0147435>

[31] Melvin, J. A., Gaston, J. R., Phillips, S. N., Springer, M. J., Marshall, C. W., Shanks, R., & Bomberger, J. M. (2017). *Pseudomonas aeruginosa* Contact-Dependent Growth Inhibition Plays Dual Role in Host-Pathogen Interactions. *mSphere*, 2(6), e00336-17. <https://doi.org/10.1128/mSphere.00336-17>

[32] Yamashita, K., Mori, A., & Otsuki, S. (1990). Changes in brain thyrotropin-releasing hormone (TRH) of seizure-prone El mice. *Experimental neurology*, 108(1), 71–75. [https://doi.org/10.1016/0014-4886\(90\)90009-h](https://doi.org/10.1016/0014-4886(90)90009-h)

[33] Allen, J. P., Ozer, E. A., Minasov, G., Shuvalova, L., Kiryukhina, O., Satchell, K., & Hauser, A. R. (2020). A comparative genomics approach identifies contact-dependent growth inhibition as a virulence determinant. *Proceedings of the National Academy of Sciences of the United States of America*, 117(12), 6811–6821. <https://doi.org/10.1073/pnas.1919198117>

- [34] Livak, K. J., & Schmittgen, T. D. (2001). Analysis of relative gene expression data using real-time quantitative PCR and the 2(-Delta Delta C(T)) Method. *Methods (San Diego, Calif.)*, 25(4), 402–408. <https://doi.org/10.1006/meth.2001.1262>
- [35] Waterhouse, A., Bertoni, M., Bienert, S., Studer, G., Tauriello, G., Gumienny, R., Heer, F. T., de Beer, T., Rempfer, C., Bordoli, L., Lepore, R., & Schwede, T. (2018). SWISS-MODEL: homology modelling of protein structures and complexes. *Nucleic acids research*, 46(W1), W296–W303. <https://doi.org/10.1093/nar/gky427>
- [36] Pincus, N. B., Bachta, K., Ozer, E. A., Allen, J. P., Pura, O. N., Qi, C., Rhodes, N. J., Marty, F. M., Pandit, A., Mekalanos, J. J., Oliver, A., & Hauser, A. R. (2020). Long-term Persistence of an Extensively Drug-Resistant Subclade of Globally Distributed *Pseudomonas aeruginosa* Clonal Complex 446 in an Academic Medical Center. *Clinical infectious diseases : an official publication of the Infectious Diseases Society of America*, 71(6), 1524–1531. <https://doi.org/10.1093/cid/ciz973>
- [37] Yajima, S., Nakanishi, K., Takahashi, K., Ogawa, T., Hidaka, M., Kezuka, Y., Nonaka, T., Ohsawa, K., & Masaki, H. (2004). Relation between tRNase activity and the structure of colicin D according to X-ray crystallography. *Biochemical and biophysical research communications*, 322(3), 966–973. <https://doi.org/10.1016/j.bbrc.2004.07.206>
- [38] Lu, S., Wang, J., Chitsaz, F., Derbyshire, M. K., Geer, R. C., Gonzales, N. R., Gwadz, M., Hurwitz, D. I., Marchler, G. H., Song, J. S., Thanki, N., Yamashita, R. A., Yang, M., Zhang, D., Zheng, C., Lanczycki, C. J., & Marchler-Bauer, A. (2020). CDD/SPARCLE: the conserved domain database in 2020. *Nucleic acids research*, 48(D1), D265–D268. <https://doi.org/10.1093/nar/gkz991>
- [39] Moon, A. F., Gaudu, P., & Pedersen, L. C. (2014). Structural characterization of the virulence factor nuclease A from *Streptococcus agalactiae*. *Acta crystallographica. Section D, Biological crystallography*, 70(Pt 11), 2937–2949. <https://doi.org/10.1107/S1399004714019725>
- [40] Boyd, A., & Chakrabarty, A. M. (1995). *Pseudomonas aeruginosa* biofilms: role of the alginate exopolysaccharide. *Journal of industrial microbiology*, 15(3), 162–168. <https://doi.org/10.1007/BF01569821>
- [41] Krasauskas, R., Skerniškytė, J., Martinkus, J., Armalytė, J., & Sužiedėlienė, E. (2020). Capsule Protects *Acinetobacter baumannii* From Inter-Bacterial Competition Mediated by CdiA Toxin. *Frontiers in microbiology*, 11, 1493. <https://doi.org/10.3389/fmicb.2020.01493>
- [42] Price, C. E., Brown, D. G., Limoli, D. H., Phelan, V. V., & O'Toole, G. A. (2020). Exogenous Alginate Protects *Staphylococcus aureus* from Killing by *Pseudomonas aeruginosa*. *Journal of bacteriology*, 202(8), e00559-19. <https://doi.org/10.1128/JB.00559-19>
- [43] Choi, K. H., Gaynor, J. B., White, K. G., Lopez, C., Bosio, C. M., Karkhoff-Schweizer, R. R., & Schweizer, H. P. (2005). A Tn7-based broad-range bacterial cloning and expression system. *Nature methods*, 2(6), 443–448. <https://doi.org/10.1038/nmeth765>

## VITA

The author, Haotian Yang, was born in Shenzhen, China on May 4, 1996 to Fengcheng Yang and Hongwei Pei. She attended the University of Washington in Seattle, Washington where she earned a Bachelor of Science in Microbiology in June 2020. After graduation, Haotian Yang matriculated into the Loyola University Chicago Stritch School of Medicine Infectious Disease and Immunology Graduate Program and began her graduate education in the Bacteriology under the mentorship of Dr. Allen. She studied the Contact-dependent Growth Inhibition of the organism *Pseudomonas aeruginosa*. After completion of her graduate studies, Haotian will pursue a job in the industry.

